

Review

# Translational Echocardiography: The Dog as a Clinical Research Model of Cardiac Dysfunction

Cesar Augusto Flores Dueñas <sup>1,\*</sup>, Ignacio Alonso Cordero Yañez <sup>2</sup>, Roberto Mujica González <sup>3</sup>,  
José Carlomán Herrera Ramírez <sup>1</sup>, Martín Francisco Montaña Gómez <sup>1</sup>, Soila Maribel Gaxiola Camacho <sup>4</sup>  
and Issa Carolina García Reynoso <sup>1</sup>

<sup>1</sup> Veterinary Sciences Research Institute, Autonomous University of Baja California, Mexicali 21360, Baja California, Mexico

<sup>2</sup> CVET, Veterinary Cardiology Services, Santiago 7910484, Chile

<sup>3</sup> Albeitar Veterinary Hospital, Guadalajara 45640, Jalisco, Mexico

<sup>4</sup> Veterinary Medicine and Zootechnics School, Autonomous University of Sinaloa, Culiacan 80260, Sinaloa, Mexico

\* Correspondence: [augusto.flores@uabc.edu.mx](mailto:augusto.flores@uabc.edu.mx)

**Abstract:** Heart disease is a major contributor to mortality and disability on a global scale. Hence, there is a need for research to improve non-invasive diagnostic techniques. Diseases in dogs with characteristics very similar to those of human pathologies hold promise as a source of data for evaluating and developing echocardiographic techniques and devices. **Methods:** We conducted a structured literature search from June 2022 to January 2023 to evaluate the relevance of dogs as a translational model for echocardiographic clinical research. We searched various academic databases, including PubMed Central (PMC), Core, DIGITAL.CSIC, DOAB, DOAJ, EBSCO host, Elsevier B.V, Redib, Scopus, and Web of Science, available through the Academic Information System of the Autonomous University of Baja California. **Results:** Out of the 243 articles initially screened, we identified 119 relevant articles that met our inclusion criteria for further analysis. This review is an introduction to the canine model by analyzing the cardiovascular anatomical similarities between the two species, the pathophysiological overlaps in some diseases, the parallels in echocardiographic techniques in dogs compared to humans, and the suitability of dogs with a naturally occurring cardiac disease as a model for translational clinical research compared to other animal species. **Conclusions:** This review emphasizes the importance of canine patients as an ideal cardiac disease symmetrical clinical model since they share common heart diseases with humans. Furthermore, dogs have a shorter lifespan, leading to the relatively rapid evolution of these diseases, which makes studying these pathologies and developing echocardiographic techniques more feasible. The results strongly indicate the need for interdisciplinary collaboration and translational medical research to create innovative echocardiographic technologies and improve the connection between veterinary and human cardiac imaging research.

**Keywords:** translational echocardiography; multidisciplinary cardiology; multidisciplinary echocardiography; comparative cardiology; comparative echocardiography; translational research; disease model



**Citation:** Flores Dueñas, C.A.; Cordero Yañez, I.A.; González, R.M.; Herrera Ramírez, J.C.; Montaña Gómez, M.F.; Gaxiola Camacho, S.M.; García Reynoso, I.C. Translational Echocardiography: The Dog as a Clinical Research Model of Cardiac Dysfunction. *Appl. Sci.* **2023**, *13*, 4437. <https://doi.org/10.3390/app13074437>

Academic Editor: Julio Garcia Flores

Received: 30 January 2023

Revised: 14 March 2023

Accepted: 15 March 2023

Published: 31 March 2023



**Copyright:** © 2023 by the authors. Licensee MDPI, Basel, Switzerland. This article is an open access article distributed under the terms and conditions of the Creative Commons Attribution (CC BY) license (<https://creativecommons.org/licenses/by/4.0/>).

## 1. Introduction

Cardiac disease is a critical global health issue affecting humans and animals, specifically domestic dogs [1,2]. Naturally occurring cardiac diseases with morphology and presentation similar to human pathologies are common in veterinary clinical settings. In addition, the similarities in cardiac diseases between humans and dogs are numerous [3]. The similarities offer a unique opportunity to obtain necessary information, and serve as a basis for clinical and research explorations of vast importance for developing improvements in diagnostic echocardiography techniques.

This review focuses on the characteristics of the most prevalent dog pathologies that are symmetrical to human cardiac pathologies in terms of pathophysiology and advanced cardiac ultrasound imaging techniques. Collaboration across disciplines can reveal new diagnostic strategies, primarily in echocardiography and therapeutics, that help approach and combat cardiovascular pathologies whose knowledge can be transferred between species. Although the use of animals in experimental research is becoming increasingly obsolete [4], clinical research is a rapidly expanding field in veterinary medicine. Furthermore, the rapid growth and short lifespan of the canine patient make it possible to study the behavior of cardiovascular diseases in a shorter period, which is advantageous for investigating the evolution of relevant pathologies.

Cardiac imaging is today an indispensable tool for diagnosis and patient evolution monitoring. In cardiology, ultrasound has broad clinical applications due to its ability to provide high-quality images, detailed descriptions, and quantifications of the cardiovascular system. An ultrasound of the heart allows the observation of mechanical, structural, and hemodynamic pathophysiological phenomena in cardiac diseases in a non-invasive manner. The improvement and evolution of diagnostic imaging would not have been possible without animal studies [5]. Current clinical veterinary cardiology uses practically the same echocardiographic techniques as human cardiology, including the most advanced techniques. In this review article, we will refer to transthoracic echocardiography (TTE).

## 2. Review Methodology

After conducting an in-depth analysis, the authors have identified four main topics and 23 subtopics that are essential to understanding the significance of dogs as a clinical model. By delving into these topics, readers can gain a comprehensive perspective on the importance of using dogs in clinical research. The present review was conducted in four steps based on the methodology proposed by [6]. Figure 1 shows the flowchart of the review process employed in this present work.

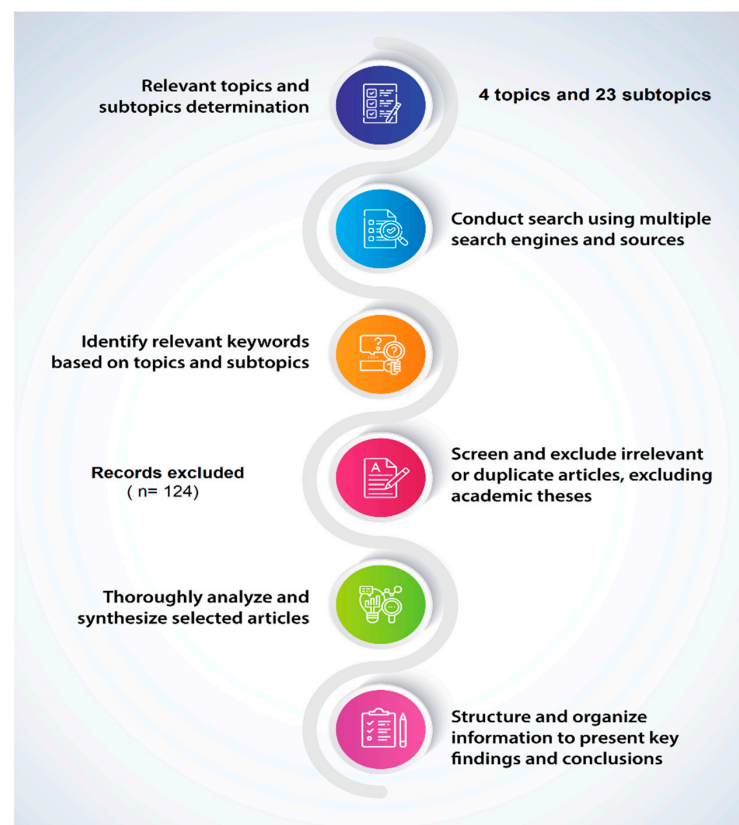
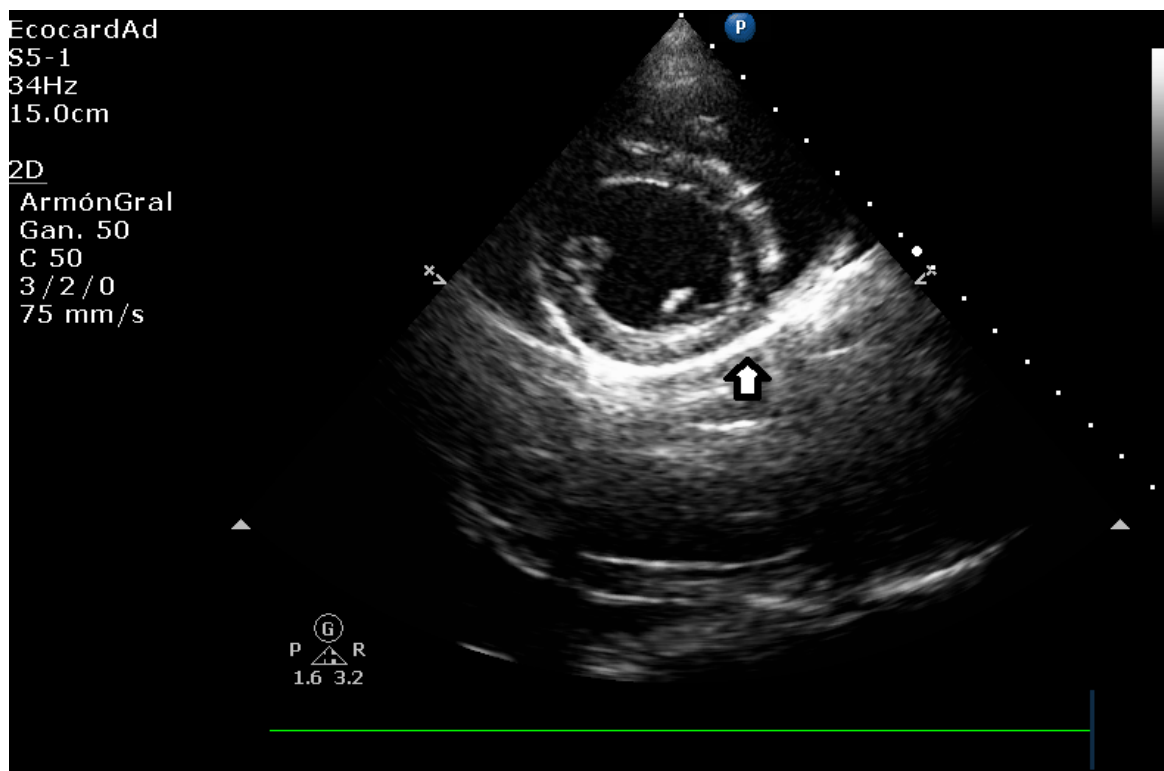


Figure 1. Review process workflow.

- Step 1. Conducting the search. The search was conducted using a comprehensive information search program that utilizes multiple search engines and information sources such as PubMed Central (PMC), Core, DIGI-TAL, CSIC, DOAB, DOAJ, EBSCO host, Elsevier B.V, Redib, Scopus, and Web of Science, available through the Academic Information System of the Autonomous University of Baja California.
- Step 2. Identification of keywords. The authors identified relevant keywords based on the four topics and 23 subtopics proposed by the authors included in this review.
- Step 3. Selection and analysis of academic information and articles. In this process, the authors screened and excluded irrelevant or duplicate articles. In this analysis, academic theses were excluded.
- Step 4. Documentation and synthesis of results. The selected articles were thoroughly analyzed and synthesized, with the information structured and organized to clearly present the key findings and conclusions.

### 3. Cardiac Anatomical Similarities between the Human and the Dog

The cardiac anatomy of dogs and humans share many similar features [3,7], as shown in Figure 2. In larger mammals such as canines, the heart is usually located ventral to the mediastinum [7,8]. Compared to humans, a dog's heart has a less pronounced left hemithorax orientation, and the long axis of the heart has a more ventral orientation. The base of the heart reaches approximately, the dorsal plane adjacent to the first rib and slopes to a variable degree in a craniodorsal direction [7,9]. Dogs have an ovoid cardiac structure [8]. This differs slightly from human anatomy, where the heart has a trapezoidal shape and, like its canine counterpart, an acute apex. In both species, the apexes of the heart consist solely of the left ventricular cavities and structures [7,9–11].



**Figure 2.** Right parasternal short axis view in the canine patient, showing pericardium as a hyperechoic line surrounding myocardium.

A dog's mean heart mass weight to body weight ratio is 0.9 to 2.2% of its body weight [10,11]. These measurements are likely to vary by breed. It has been reported that a human's mean heart mass weight to body weight ratio is 5 g per kilogram [11].

The pericardium surrounds the heart in humans and dogs, creating the pericardial cavity. The pericardium is attached to the diaphragm and sternum at the base of the heart. However, both species have different degrees of attachment to the diaphragm [8,12,13]. Humans have a firm and broad extension to the central tendinous aponeurosis of the diaphragm. On the other hand, dogs have a phrenopericardial ligament attached to the pericardium and, externally, a thin layer of mediastinal pleura attached to the pericardium, allowing the heart to be kept centered in the thorax [11].

The basic structure of the pericardium is very similar between the two species, but there are distinct differences [14–16]. Unlike other large mammals, where the thickness of the pericardial wall increases with heart size, humans have a thicker pericardium than animals with similar heart sizes [11]. In the human heart, the thickness of the pericardium is 2 mm or less [17], whereas the thickness of the pericardium in the dog is considerably thinner (0.18–0.20 mm) [11]. The normal pericardial fluid volume in most dogs is between 0.5 and 2.5 mL, and some dogs may have up to 15 mL, compared to volumes of 20–60 mL in adult human hearts [11–13].

### 3.1. Auricular Anatomical Coincidences

Similar to humans, the right and left atria of the adult dog heart are separated by the interatrial septum a muscular wall that extends from the base of the heart to the atrioventricular valves. The interatrial septum is composed of two layers: the muscular layer, which is continuous with the myocardium of the atria, and the membranous layer, which is a thin fibrous membrane that covers the muscular layer [7,11]. The cardiac base receives all the great vessels. It is generally cranially oriented and in mammals, including dogs, the orientation of the cardiac base is primarily determined by the animal's posture [9,13]. Recent studies suggest that cardiac orientation also varies with age and other factors, such as body size and physical activity [18]. Additionally, advances in imaging technology have allowed for more detailed visualization and understanding of the complex anatomical structures of the heart [19]. Symmetrically to humans, during fetal development, the human heart is structured to allow blood to flow directly from the right to left atrium, bypassing the lungs. This occurs via the foramen ovale, which is a small opening in the interatrial septum. The foramen ovale has a valve-like flap on the left atrial side, which prevents blood from flowing back into the right atrium when the left atrium contracts. Once the newborn begins to breathe air, the pulmonary circulation is established, and the foramen ovale usually closes, becoming a small depression in the interatrial septum known as the fossa ovalis [11,19]. In adults, the fossa ovalis is a slight depression on the right atrial side of the interatrial wall [13,19]. Dogs have more posterior fossa ovalis than humans [7].

In large mammals, the venous sinus is integrated into the right atrium and marked by the sinoatrial node. Dogs have the same atrial architecture, which includes the venous sinus, crista terminalis, fossa ovalis, and Eustachian valves (inferior vena cava and coronary sinus valves) [9,13]. Normally, there is an anterior (cranial or superior) and a posterior (caudal or inferior) vena cava. The location of the vena cava ostia entering the atrium may vary in some mammals [7,11,19]. Specifically, the inferior and superior vena cava ostia enter almost at right angles in animal models of large mammals, whereas in humans, they enter the atrium almost in line [9,11]. The inferior vena cava in domestic animals is usually long (>5 cm) in contrast to its short length in humans (1–3 cm) [7,11]. In most species, the coronary sinus ostium is located in the posterior wall of the right atrium, but its location may vary slightly. There are also considerable species differences in the number of pulmonary veins entering the left atrium. In human hearts, there are four [9,20,21] or occasionally five pulmonary veins, whereas in dog hearts, there are five or six [11]. In large mammals, the atria are separated from the ventricles by a fibrous tissue called the cardiac skeleton. The cardiac or fibrous skeleton is composed of dense connective tissue and consists of four fibrous rings that encircle the four heart valves - the mitral valve, tricuspid valve, aortic valve, and pulmonary valve. These rings provide support for the heart valves and help to maintain their proper position. In addition to the fibrous

rings, the cardiac skeleton also contains fibrous tissue that forms a barrier between the atria and ventricles. This barrier prevents the electrical signals that control the heart's contraction from spreading between the atria and ventricles, ensuring that the heart beats in a coordinated manner. The fibrous skeleton also serves as an attachment site for the heart's muscle fibers and for the connective tissue that surrounds the heart [11,22].

### 3.2. Ventricular Chambers in Both Species

With characteristics common to the human heart, the ventricles are the main ejection chambers of the heart. Therefore, their walls are much more muscular than the atria, making this normal function more efficient. Since the wall thickness of the right ventricle corresponds to approximately one-third of that of the left ventricle, the structure results in lower systolic pressure. The left ventricle exhibits a greater degree of muscularity compared to the right ventricle. This is because the left ventricle has to generate high pressure to propel blood through the systemic circulation, which comprises a larger network of blood vessels compared to the pulmonary circulation. In fact, systemic circulation has a resistance that is usually more than four times higher than pulmonary circulation, necessitating a greater contractile force in the left ventricular wall. To achieve efficient contraction of the heart, trabeculae are interlaced between the walls of both ventricles, primarily near the apex, thereby reinforcing the walls and increasing the force of systolic contraction. This intricate network of trabeculae, known as the trabecular network, plays a crucial role in maintaining the structural integrity and functionality of the heart [11,13]. Larger mammalian hearts have less ventricular trabeculation than normal adult human hearts, and the trabeculations are usually thicker than human hearts as a compensatory contractile phenomenon [7,9,11]. In dogs, the walls of the ventricles are attached to papillary muscles that support the atrioventricular valves.

The heart of a large mammalian animal, such as a dog, has three papillary muscles in the right ventricle and two in the left ventricle, similar to human anatomy. However, variations occur in individuals and species [7,8,11]. There are at least two chordae tendineae per papillary muscle to ensure redundancy. Both ventricles are traversed by fibrous or muscular bands containing Purkinje fibers. The dog's right ventricle usually has a prominent moderator band [7]. Species differ significantly in the origin and insertion of the band, as well as in its structure. In the dog, the septal wall near the base of the anterior papillary muscle extends into the lumen through one or more branched muscle filaments. Dogs' left and right ventricles are also structurally symmetrical to human chambers. At the opening of the septal leaflet of the mitral valve, the dog's left ventricle physiologically divides into an inflow and outflow region, exhibiting a conical structure [11,19].

### 3.3. Similarities in Cardiac Valves

The dog heart has four cardiac valves with structures and locations similar to humans. As illustrated in Figure 3, its transthoracic echocardiographic appearance and other cardiac structures are similar to that of humans. The heart has two atrioventricular valves and two semilunar valves situated between the ventricles and the outflow tracts of the pulmonary artery and aorta on either side. These valves play a critical role in regulating the flow of blood through the heart. The fibrous leaflets of the atrioventricular valves are connected to the papillary muscles of each ventricle by the chordae tendineae. This connection is essential in preventing atrial valve prolapse during ventricular contraction. On the other hand, the closure of the pulmonary, semilunar, and aortic valves does not involve chordae tendineae but instead relies on pressure gradients to facilitate their proper functioning [11,19].

In both dogs and humans, the tricuspid valve separates the right atrium from the right ventricle and is almost symmetric in structure. The right ventricle has three papillary muscles associated with it. In some cases, the anterosuperior and inferior leaflets of the tricuspid valve may appear to have only two leaflets in certain canine patients due to the fusion of their commissures [11]. Variations in the number of papillary muscles have been observed not only between different mammalian species but also among individuals

within the same species. These variations are important to consider when evaluating cardiac function and diagnosing any abnormalities or pathologies. The left atrium and left ventricle are separated by the bicuspid valve, which typically has two leaflets—anterior or septal and posterior or parietal. However, it has been reported in humans that the mitral valve may have multiple leaflets, with some individuals exhibiting significant variations in the number and morphologic variability of the mitral valve leaflets [23]. This anatomical variation is relatively rare, but it is important to be aware of it when evaluating mitral valve function or performing interventions on the valve. In both humans and dogs, there is a fibrous connection between the mitral and aortic valves that extends from the central fibrous body to the left fibrous trigone. This fibrous continuum is important for maintaining the structural integrity of the heart and for the proper functioning of the valves [7]. There are variations in the annulus fibrosus that support the mitral valve and its leaflets among different species. In humans, there is an annular segment at the base of the mural cusp. However, this segment can be difficult to identify in some breeds of dogs [11]. The semilunar pulmonary valve has a similar appearance to the aortic valve but is thinner. Unlike the aortic valve, there are no coronary ostia located behind the cusps of the pulmonary valve [7].

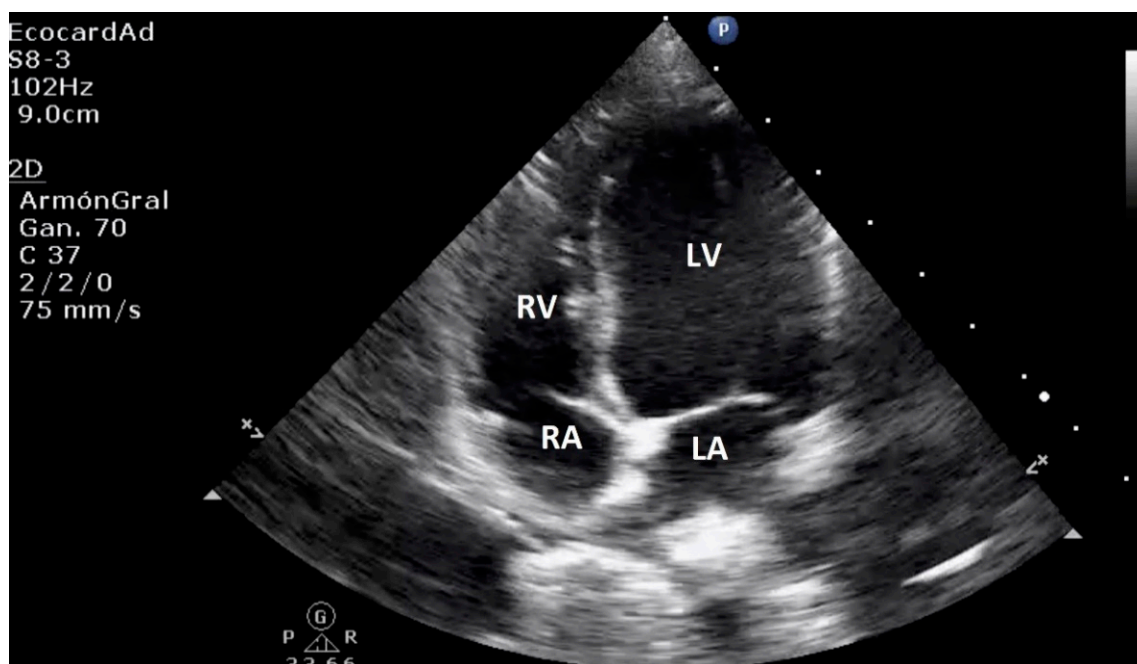


**Figure 3.** Right parasternal 4 chamber apical view demonstrates left and right ventricle, left and right atrium, and atrioventricular valve.

### 3.4. The Coronary System

In mammals, the intrinsic circulatory system consists of two main coronary arteries [7]; the coronary sinus is an essential pathway that connects the coronary veins to the right atrium. It is a complex network of tributary veins that returns deoxygenated coronary blood to the right atrium. Positioned posterior to the coronary sulcus, the coronary system has an orifice located in the medial and anterior area of the inferior vena cava's orifice. It is located immediately above the atrioventricular junction. A semicircular valve, known as the valve of Thebesius, guards the orifice of the coronary sinus, which is always located in the morphologic right atrium in a healthy individual [24]; The perfusion areas of large mammals differ between and within species; similar differences have also been described in humans. Dogs usually receive most of their myocardial supply from the left coronary artery, whereas in roughly 90% of human cases, the right coronary artery is dominant [11]. Normal human hearts show little development of coronary collateral circulation [25]. In contrast,

canine hearts present extensive coronary collateral networks located almost exclusively on the epicardial surface [11,26].

#### 4. Myxomatous Mitral Valve Disease in Dogs as a Clinical Model in the Study of the Pathology in Humans

Myxomatous degeneration of the heart valves (MDMV) or myxomatous mitral valve disease (MMVD), which occurs in both canine and human patients, is a non-inflammatory pathology with a continuous progression of the valvular structure caused by a defect in the mechanical integrity of the leaflets as a result of altered synthesis and remodeling, and the continuous wear they receive as part of the disease mechanism. The presence of bulky and thickened valve leaflets is some of the most characteristic morphological abnormalities detectable by echocardiography (Figure 4). In addition, this pathology affects valvular and chordae tendineae integrity, which likewise shows thickening, elongation, and instability, and may rupture [27–29].

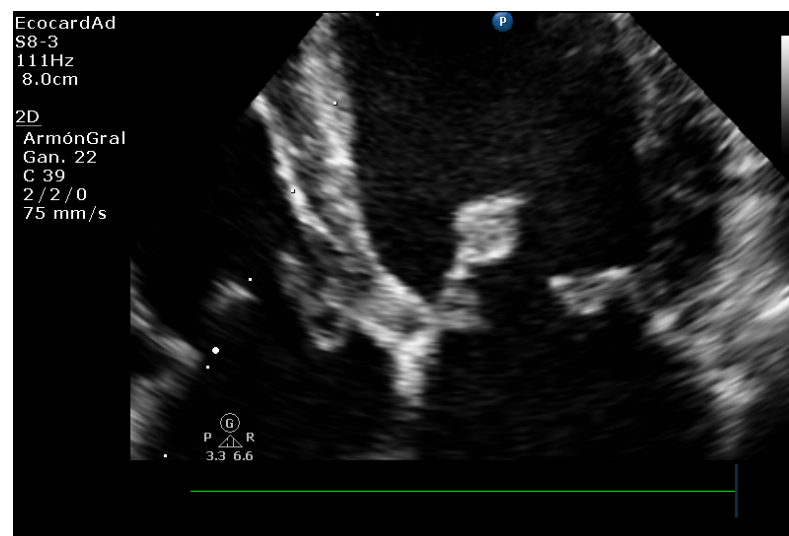


**Figure 4.** Myxomatous mitral valve degeneration in the canine patient's left apical 4-chamber view.

One of the main objectives of this review is to highlight the potential value of natural MMVD in the dog as a model for interdisciplinary echocardiographic clinical research.

#### 5. (MDMV) Comparative Pathology and Pathophysiology

The mitral valve structure undergoes severe and repeated mechanical stress during systole, the pressure generated by the contracting left ventricle causes the valve leaflets to close, resulting in mechanical stress on the valve structure. The fibroblasts and myofibroblasts in the valve tissue respond to this stress by synthesizing and remodeling the extracellular matrix, which is the network of proteins and other molecules that provide support and structure to the valve tissue. This remodeling process involves the deposition of new extracellular matrix components, such as collagen and elastin, and the breakdown of old or damaged components. During diastole, the pressure in the left atrium decreases, and the valve leaflets open, resulting in flexion of the valve structure. The smooth muscle cells and interstitial cells in the valve tissue respond to this mechanical stress by contracting and relaxing, respectively, to help maintain the valve's shape and function. Furthermore, the endothelial cells that line the inner surface of the valve leaflets experience shear stress from the blood flow. These cells respond to this stress by releasing signaling molecules that regulate cell behavior and extracellular matrix synthesis, helping to maintain the valve's integrity and function [30,31]. The above occurs when the heart valves open and close more than three billion times in the half-life of a human adult and more than half a billion times in the half-life of a canine.

The mitral apparatus experiences the cardiac apparatus's most significant transvalvular pressure gradient [30]. During the contractile phase, the leaflets endure high degrees of tension and rapid mechanics of movement and stretching, constant tension, and, after complete closure, an extreme increase in tension and stiffness to avoid further deformation of the leaflets, and prevent the mitral regurgitation caused by the straightening of the collagen fibers within the leaflets [32,33].

The macroscopic and histological structures of the human and canine leaflets are similar [34,35] and are designed to withstand repeated stresses due to the specialized structure of the inner layers of the mitral leaflets [30,34,35]. The mitral valve is closely related to the fibrous skeleton of the heart, and the mitral annulus, in particular, is an important component of the fibrous skeleton that helps to maintain the shape and function of the valve [30,36]. The valvular annulus is the ring-like structure that supports the mitral valve and connects it to the heart's muscular wall. It serves as an anchor for the valve's leaflets, chordae tendineae, and papillary muscles, allowing for the proper opening and closing of the valve during the cardiac cycle. The shape of the valvular annulus is not flat but rather saddle-shaped, with a higher curvature at the anterior and posterior ends and a lower curvature at the lateral ends. This shape reduces the stress on the chordae tendineae and leaflets during systole when the valve is closed, as it allows for the distribution of the mechanical forces evenly across the valve. The saddle-shaped annulus also enables the valve to open and close more efficiently, reducing the strain on the valve and its components [30,37,38]. Other similarities of the mitral valve structure in dogs and humans include the continuity of the anterior leaflet with the aortic valve cusps at the aortic root and a branched network of chordae tendineae that connects to the anterior and posterior papillary muscle [19].

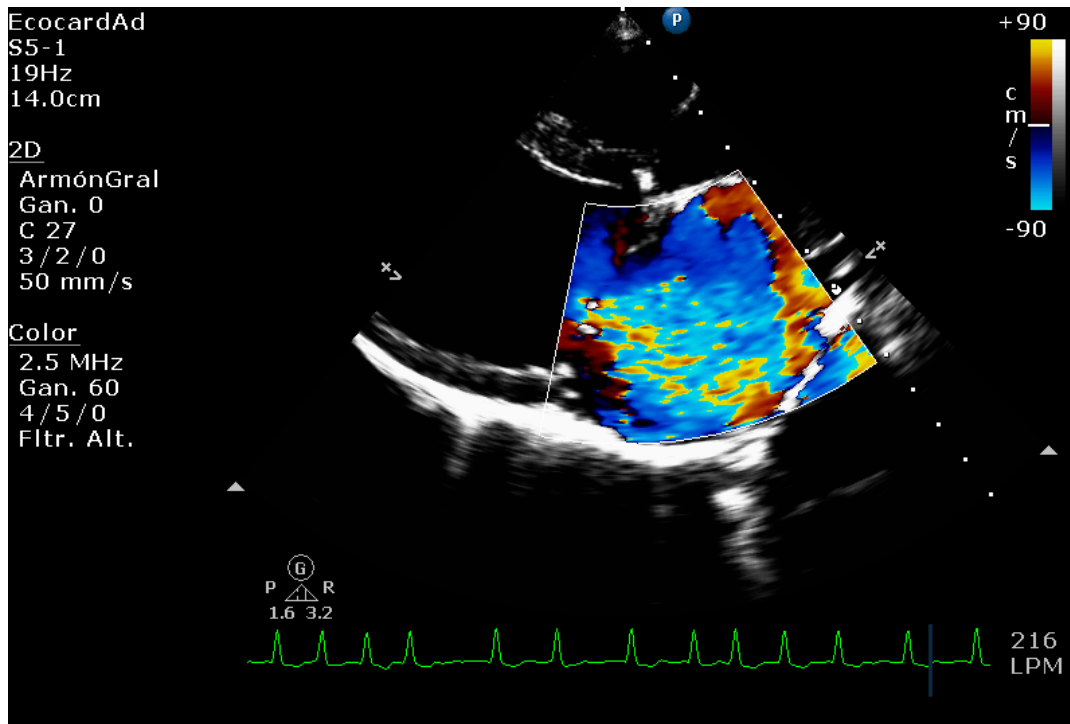
The mitral apparatus, which is present in both humans and dogs, consists of layers of extracellular matrix and connective tissue. The specialized innermost regions include a spongy region made of an extracellular proteoglycan matrix and a fibrous region composed of collagen that extends to the chordae tendineae. Valvular interstitial cells are also present in the valve [30,39–41]. Valvular interstitial cells are crucial for maintaining the structure and function of the mitral valve. They regulate the composition of the spongiosa and fibrosa to ensure proper balance between synthesis and degradation of extracellular matrix components. This helps maintain the integrity of the valve. The spongiosa, which is rich in proteoglycans, allows for absorption of large forces and stresses during closure. The leaflets of the valve are further reinforced by layers of collagen and elastin, which provide the necessary tensile strength during closure [30,39,42].

Some forms of mitral valve disease in humans and dogs involve the thickening of the leaflets and nodular growths along their edges, resulting in valvular insufficiency. Additionally, the expansion of the spongiosa and loss and disorganization of the collagen fibers in the fibrosa layer can lead to the rupture of the chordae tendineae [30,39] (Figure 5a,b).

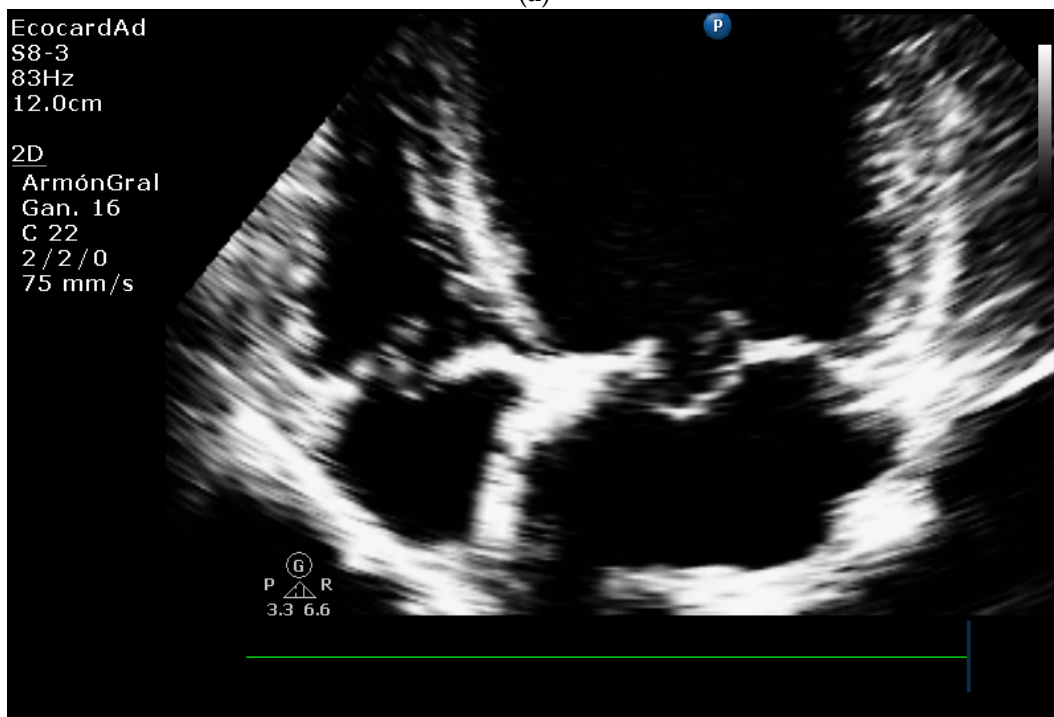
Myxomatous mitral valve regurgitation is the most common type of valvular heart disease, affecting 0.6–2.4% of the population, and is the leading indication for surgical repair of the mitral valve in humans [30,43,44]. This condition is also known as myxomatous mitral valve disease or mitral valve prolapse syndrome. Understanding the pathophysiological mechanisms of this valvular lesion is crucial to manage this disease. Analyzing echocardiographic changes during the disease can help provide a better understanding of the disease and help stratify the risk in different populations of patients with this pathology.

The timely diagnosis of mitral valve prolapse syndrome and the determination of the ideal moment for its surgical correction is an essential factor in clinical cardiology. Chronic mitral regurgitation, due to the increasing average age of the population and the higher prevalence of myxomatous disease in the human population, occurs as frequently as aortic stenosis. Moderate or severe mitral regurgitation is found in 1.7% of the population worldwide and up to 9.3% of geriatric patients older than 75 years [44–46]. Echocardiographic techniques are the main tool for the evaluation of mitral regurgitation. In the current medical environment, echocardiography is more important than ever for diagnosing valvular

pathology that causes mitral regurgitation phenomena of varying severity and determining the timing of medical or surgical intervention. Important clinical indicators related to the stage of mitral regurgitation include patient symptoms, echocardiographic findings, and hemodynamic indicators, allowing cardiologists and cardiac surgeons to conduct a comprehensive assessment for optimal clinical outcomes [44].



(a)



(b)

**Figure 5.** (a) Mitral insufficiency and (b) Septal leaflet prolapse associated with Myxomatous degeneration in a canine patient.

### 5.1. Mitral Valve Disease Epidemiology

Mitral regurgitation is a common valvular heart disease affecting millions of people worldwide. It is the third most common form of valvular heart disease, and its prevalence is estimated to be between 3–5% in the general population. Mitral valve prolapse is the most common mitral valve pathology, accounting for 2% to 3% of the total population [45]. The chronic degenerative nature of this pathology and the increased life expectancy probably contribute to these presentation rates [46]. Degenerative myxomatous mitral valve disease is dogs' most prevalent form of heart disease. In the same way, being a degenerative phenomenon, it is more present in geriatric patients [30,47].

Degenerative myxomatous mitral valve disease is commonly observed in other small dog breeds with less than 15 kg of body weight, such as Miniature Poodles, Miniature Schnauzers, and Chihuahuas [48–52]. In fact, this pathology accounts for a substantial proportion of all heart disease cases in dogs, amounting to around 75% of cardiac clinical cases [51].

Mitral valve prolapse is a condition commonly observed in Cavalier King Charles Spaniels, characterized by the failure of the left atrioventricular valve to close properly due to the accumulation of abnormal myxomatous material and nodular changes on the valve leaflets. This condition is prevalent in a significant percentage of Cavalier King Charles Spaniels, ranging from 11.4–44.95%, and is often accompanied by age and sex-dependent heart murmurs. This degenerative valve disease is similar to myxomatous valvular degeneration, also known as valvular endocardiosis. Although tricuspid valve involvement is less frequent, it can still occur. What makes Mitral valve prolapse in Cavalier King Charles Spaniels unique is that it tends to occur at a younger age, with almost 19% of dogs under one year of age exhibiting heart murmurs, and likely more than 50% of dogs over five years of age displaying murmurs [50,51].

Degenerative mitral valve disease is a prevalent cardiac condition affecting dogs and humans, characterized by progressive degeneration of the mitral valve leading to mitral regurgitation. The clinical presentation varies in both species and can range from mild asymptomatic regurgitation to severe mitral insufficiency with congestive heart failure [52]. In dogs, valvular degeneration, mitral regurgitation, eccentric cardiac hypertrophy, systolic dysfunction, left heart failure, and congestive heart failure are the clinical consequences of severe Degenerative mitral valve disease. In addition, Cardiac mortality within six years of diagnosis of mitral valve disease is 11% in dogs [53,54]. Although surgical repair is associated with better outcomes, it is not widely available due to its high cost and the limited number of veterinary medical units that perform the procedure. Therefore, medical treatment with loop diuretics, Angiotensin-converting enzyme inhibitors, aldosterone receptor inhibitors, and inodilators or positive inotropes is the standard of care for dogs with severe mitral regurgitation and secondary congestive pulmonary edema [30,54,55].

The clinical course of Degenerative mitral valve disease in dogs begins with mild asymptomatic mitral regurgitation, progresses to varying degrees of mitral insufficiency with eccentric left ventricular hypertrophy and atrial enlargement, and commonly escalates later to severe mitral insufficiency with clinical signs of congestive pulmonary edema, typically occurring during the relatively short adult lifespan of the dog compared to humans [30].

### 5.2. Canine Myxomatous Mitral Valve Disease. Comparative Transthoracic Echocardiography with Human Mitral Valve Prolapse

Many diagnostic methods exist for evaluating mitral valve disease in human and small animal medicine. Transthoracic echocardiography is a basic and primary test for establishing both species' diagnosis and prognostic profile of mitral valve disease. TTE enables clinicians to identify mitral valve lesions, classify the extent and type of regurgitation, evaluate the severity of cardiac remodeling, assess myocardial function, and measure left ventricular filling pressures and pulmonary artery pressure, providing a comprehensive evaluation of cardiac health [56–58]. Various types of ultrasound imaging technologies are

available and frequently employed in veterinary and human cardiology. These include traditional methods such as two-dimensional (2D) Doppler echocardiography, M-mode, color Doppler, pulse wave (PW), continuous wave (CW), as well as newer and more advanced techniques such as tissue Doppler (TDI), two-dimensional speckle tracking echocardiography (STE), and strain and strain rate ultrasound. These echocardiographic techniques in parallel settings can assess and monitor regional and global myocardial function and stratify the severity and progression of mitral valve pathology [59–61]. While the evaluation of mitral regurgitation and chronic heart failure severity in dogs with mitral disease shares similarities with that in human patients, veterinary cardiologists prioritize assessing the extent of cardiac remodeling and dysfunction as a result of mitral regurgitation.

### 5.3. Comparative Assessment of Mitral Regurgitation Severity

In order to assess the severity of a valvular defect, color flow and continuous wave signals of mitral regurgitation jets (CW) are utilized in both humans and animals. Still, a more quantitative approach is required on both species to determine mitral regurgitation severity. This quantitative assessment is commonly used in humans to grade the severity of mitral regurgitation [61]. Although a quantitative assessment of mitral regurgitation (MR) is commonly used to grade the severity of MR in human patients, it is seldom utilized in veterinary medicine. This is because the practical application of this method is limited in dogs, and defining the location of effective regurgitant orifice area (EROA) and the flow convergence shape in canine patients with mitral regurgitation can be challenging [60].

### 5.4. Mitral Regurgitation Quantification in the Canine Model

The Proximal Isovelocity Surface Area (PISA) method is a widely accepted gold standard for quantifying the extent of mitral regurgitation jet in humans [60,61]. While a clinical study has shown that this method is repeatable and reproducible in awake dogs [62], it is less practical and requires several precautions to obtain optimal flow convergence images in dogs with mitral disease [63,64]. Therefore, in veterinary practice, the use of PISA should be employed with caution, taking into account the potential limitations and technical challenges associated with its application. The severity of mitral regurgitation in dogs can be determined by the regurgitation fraction (RF) obtained through the proximal isovelocity surface area (PISA) method. Several studies have demonstrated that RF is closely associated with the severity of degenerative valve disease and other important echocardiographic indicators, such as the ratio of the left atrium to the aorta (LA/Ao) and pulmonary artery systolic pressure [62,65]. A different clinical study found that PISA quantification of mitral regurgitation showed a wide range of RF, which is why it is not routinely performed in cardiologic evaluation in dogs [62].

The severity of mitral regurgitation can be semi-quantified using color-flow Doppler to measure the mitral regurgitant maximum jet area (MRA) ratio in relation to the left atrial area (LAA). This method has been validated in dogs and demonstrates a strong correlation with Doppler-derived regurgitant volume and effective regurgitant orifice area, making it a reliable tool for assessing mitral regurgitation severity [66,67]. In human medicine, mitral regurgitation has been widely studied, and there are several stratification scales and widely disseminated echocardiographic evaluation guidelines [61,68,69]. In the same way, as in TTE studies of canine patients, the characteristics and changes in mitral structure and morphology and signs of valvular remodeling are evaluated. Doppler technology is also useful for assessing mitral regurgitation qualitatively, semi-quantitatively, and quantitatively.

Most of the echocardiographic variables used in the human patient have been studied in domestic canine medicine; in the same way, these methods require extensive training to obtain repeatable results in the measurements and avoid measurement variability in the generation of erroneous results [70]. Color flow imaging of the mitral regurgitation jet area is the most commonly used technique for assessing the severity of mitral regurgitation in dogs. The former method is not used in humans, as it is not considered reliable for determining the severity of mitral insufficiency [68,69]. This method has become widespread in the

domestic canine patient because it is easy to perform; however, some studies have indicated that the correlation of the jet area with the severity of mitral regurgitation is poor, as well as its reproducibility [67]. One of the most commonly used semiquantitative techniques in veterinary TTE is the measurement of the effective regurgitant orifice or the width of the vena contracta. This method, compared with other qualitative methods, is equally useful for evaluating eccentric and central jets. However, it is unreliable in multiple jets as it depends on the geometry of the regurgitant orifice [69]. A study in dogs with Mitral Myxomatous Degeneration reported that vena contracta and E-vel correlated strongly with mitral regurgitant fraction reported in cardiac MRI studies.

However, E-vel had superior repeatability, being more reliable in dogs [71]. Among quantitative methods, proximal isovelocity surface area assessment is one of the most widely used methods to evaluate the effective regurgitant orifice area and regurgitant volume. However, its reliability in eccentric jets has been questioned [69,72]. Another important fact is that echocardiographic dynamic behavior and variability of mitral regurgitation in patients with mitral valve prolapse has been described in dogs, which should be considered an inherent limitation of the proximal isovelocity surface [73]. Different authors have described real-time three-dimensional echocardiography as a useful tool to evaluate the effective area of the regurgitant orifice in dogs with MMVD [73,74]. The above technique is not widely used due to the need for highly trained personnel and high equipment costs for its implementation in clinical veterinary practice. Other quantitative methods based on spectral Doppler for assessing effective regurgitant orifice areas and regurgitant volumes, such as the mitral inflow method and systolic volume requirement, are impractical in veterinary medicine, and humans are not recommended as a first-choice method for quantifying the severity of mitral regurgitation [68,69,71].

The clinical stage classification of canine patients with MMVD should be based on ACVIM guidelines, which recommend using LA/Ao and LVIDDn to determine the degree of cardiac remodeling [55]. A study involving 558 dogs with MMVD found that LA/Ao > 1.7 was the most significant prognostic index among the echocardiographic indices currently used in veterinary cardiology [75]. Recently, a specific score, the proposed MINE score, relies on four distinct echocardiographic indicators [70]: (1) the left atrium to aorta (LA/Ao) ratio is determined from the right parasternal short-axis view [76]; (2) the left ventricular end-diastolic diameter is adjusted for body weight to obtain a normalized value. This approach allows for a more accurate interpretation of the data, since the size of the left ventricle can vary significantly based on the size of the animal (LVIDDN), obtained in M-mode and in the right parasternal short-axis projection [77]; (3) the left ventricular shortening fraction (FS) is obtained in M-mode obtained in the right parasternal short-axis window [77]; and (4) the maximum velocity of the E-wave transmitral flow (E-vel) is commonly obtained using pulsed Doppler imaging in the left apical four-chamber projection [78]. The above protocol has been proposed as a staging tool for the severity of myxomatous mitral valve disease in dogs. For the purpose of evaluating left-sided cardiac remodeling, left ventricular dynamics, and left ventricular filling pressure, the authors of this study selected four key echocardiographic variables [70]. These variables include LA/Ao and LVIDDN for the assessment of left cardiac remodeling, FS for left ventricular function, and E-vel for evaluating left ventricular filling pressure, all of which are echocardiographic variables evaluated in the mentioned study. The MINE scores have prognostic value in dogs with myxomatous mitral valve disease.

##### *5.5. Left Heart Remodeling Assessment and LA Evaluation*

Chronic, hemodynamically significant mitral regurgitation can lead to volume overload of the left atrium (LA) and left ventricle (LV), resulting in the enlargement of both chambers of the heart. To assess the severity of LA and LV remodeling, several indicators can be evaluated, including the LA-to-aortic root ratio (LA/Ao), indexed LA diameter, LV end-diastolic internal dimension to aortic root ratio (LVID/Ao), and LV internal dimension at end-diastole (nLVID). These parameters can provide valuable information about the

degree of cardiac remodeling and guide management decisions for patients with chronic mitral regurgitation [36].

Estimating the diameter of the left atrium (LA) is a highly reliable indicator of prognostic outcomes in dogs with mitral valve disease (MMVD) [54]. It also enables the decision to initiate medication in dogs with preclinical MMVD and to estimate the risk for the development of left-sided congestive heart failure (CHF) [79]. When evaluating dogs with MMVD, assessments of left atrial and left ventricular chamber dimensions can aid clinicians in predicting the likelihood of disease progression and the risk of developing congestive heart failure [79,80]. The extent of left atrial enlargement is significantly associated with the progression of congestive heart failure and the survival rates of both symptomatic and asymptomatic dogs with MMVD [57,65].

### 5.6. Comparative Left Ventricle Assessment

Systematic left ventricle evaluation provides important information to assess the severity and progression of degenerative mitral valve disease. The mechanisms involved in LV remodeling and enlargement resulting from mitral regurgitation are a set of complex mechanical wear and tear mechanisms and cellular and structural responses to that stress [81], leading to a progressive increase in end-diastolic and end-systolic volume. Research in canine patients identified an allometric relationship between body weight and LV end-systolic diameter (LVID) and LV end-diastolic diameter (LVIDd) in the M-mode approximation [82], which now allows prediction intervals to be determined for a wide range of canine patients' body weights. It was standardized that using the dimensions of the LVIDd in M-mode divided by the body weight of the dog raised to the power of 0.294 ( $BW^{0.294}$ ) should be found in the reference values of  $\leq 1.85$ , in addition to the LVID values obtained in M-mode divided by the body weight of the dog raised to the power of 0.315 ( $BW^{0.315}$ ) must be in the cutoff point of  $\leq 1.26$ ; values greater than these indicate LV enlargement in the canine patient. There are scenarios where the systolic function can be affected in dogs with MMVD [82]. However, the evaluation of systolic function in dogs presents challenges in its assessment due to the change in ventricular load conditions. With disease progression, mitral regurgitation results in a gradual increase in preload and a slight decrease in afterload. There is a significant impact on all non-invasive indicators of cardiac function as a result of these changes. A hyperdynamic ventricle commonly increases fractional shortening and ejection fraction, reducing its sensitivity for detecting LV dysfunction in patients with this pathology [83]. With this pathology, increased left ventricular dimensions at the end of systole could indicate a decrease in systolic function. Considering the relationship between this measurement and patient weight, an allometrically scaled  $LVID > 1.26$  suggests an increase in LVIDs, which may indicate LV systolic dysfunction in patients with MMVD [82].

### 5.7. Key Main Useful Echocardiographic Considerations for the Approach of Mitral Endocardiosis in Canine Patients

#### 5.7.1. Evaluation of the Regurgitant Area

It corresponds to a semi-quantitative analysis that evaluates the route of the regurgitant flow. For example, in the left apical four-chamber or right parasternal four-chamber view, the color Doppler mode will allow us to obtain its area, called the regurgitant jet area (Figure 6), and compare it with the area of the left atrium.

This technique is a reliable diagnostic approach with good repeatability and reproducibility when performed by a trained clinician. It can be used to assess the severity of mitral regurgitation by measuring the regurgitant volume and calculating the regurgitant fraction. A regurgitant fraction of less than 30% indicates mild mitral regurgitation, while a regurgitant fraction between 30% and 70% indicates moderate regurgitation. A regurgitant fraction greater than 70% indicates severe regurgitation. However, it is important to note that this method has limitations. The accuracy of the measurements is influenced by factors such as systolic blood pressure, left atrial pressure, jet direction, the frequency of the

transducer, and the gain level. Clinicians should be aware of these limitations and use their clinical judgment when interpreting the results. In some cases, additional diagnostic tests or assessments may be necessary to fully evaluate the severity of mitral regurgitation [84,85].

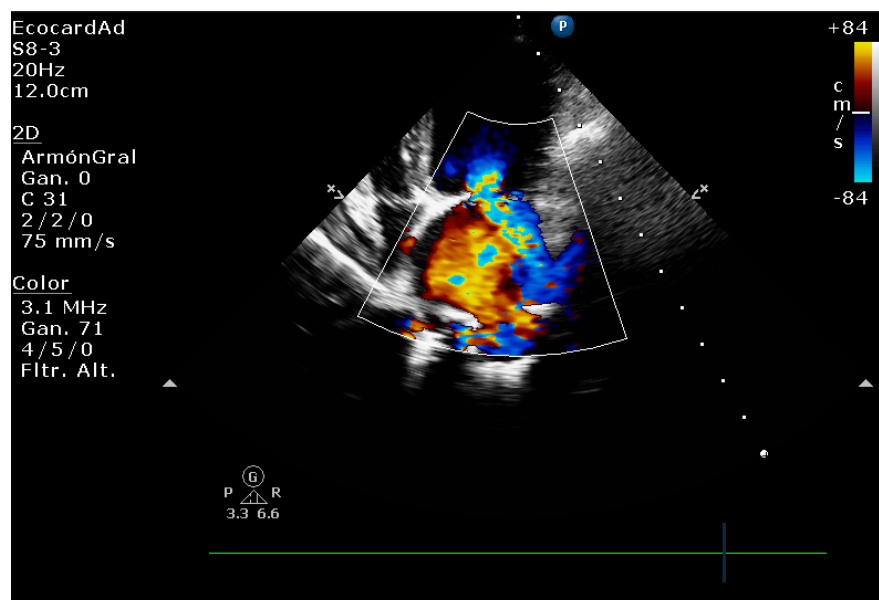


**Figure 6.** Severe mitral regurgitation in the canine patient.

#### 5.7.2. Presence of Vena Contracta

The vena contracta is a simple and reproducible method. It is defined as the narrowest area of the regurgitant jet, immediately below the anatomical orifice, as shown in Figure 7. The width correlates with the size of the regurgitant orifice. It is measured in the parasternal long axis or apical planes, moving the color baseline in the direction of the jet up to a Nyquist velocity that identifies the narrowest area of the jet (40–70 cm/s). Other methods must be used for intermediate values or multiple jets [54,85,86].

#### 5.7.3. Degree of Myxomatous Degeneration

Nodules appear at the free edges of the leaflets with myxomatous degeneration, along with the thickening of the chordae tendineae, as shown in Figure 8. The nodules can fuse as they enlarge, resulting in a generalized mitral valve thickening. A rupture of the chordae tendineae can cause the valve to lose its support, further aggravating regurgitation. These abnormalities have different consequences depending on their deformation, retraction of valve leaflets, and chordae tendineae condition [82,84,85,87–89]. The mitral valve leaflets appear remodeled and thickened in a two-dimensional mode, with an irregular nodular appearance.

#### 5.7.4. Mitral Valve Prolapse

It is characterized by the movement of one or two leaflets beyond the annular plane of the mitral valve in systole. When the chordae tendineae rupture, all or part of the affected leaflet usually prolapses into the left atrium in systole. The severity of the prolapse correlates with the stage of mitral regurgitation. The rupture of the chordae tendineae corresponds to a relevant situation since they determine the final systolic position and tension of the mitral valve leaflets, and contribute to the systolic closure of the mitral valve. Myxomatous degeneration can lead to chordae tendineae rupture, aggravating pre-existing mitral regurgitation [84,85,87,88].

Primary rupture of the chordae tendineae can lead to a complete loss of tension in one of the leaflets, which generates a movement that shows the dance of the chordae tendineae, known as “flail”. This event leads to an abrupt worsening of mitral valve regurgitation,

which in the worst case, will cause acute congestive heart failure (CHF). Ruptured chordae tendineae can be seen using traditional two-dimensional TTE, as shown in Figure 9 [84,85].

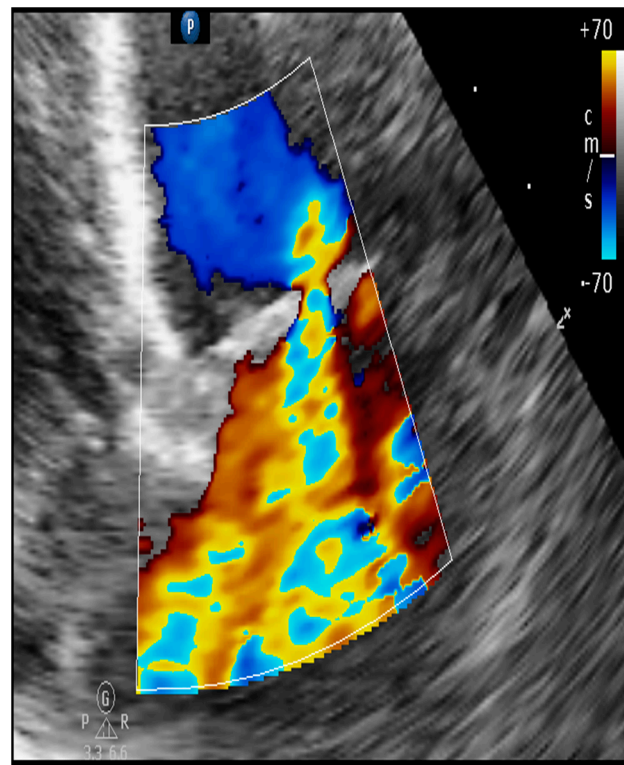


**Figure 7.** Mitral regurgitation due to myxomatous degeneration with severe regurgitation. The presence of vena contracta that demonstrates greater severity is associated with non-coaptation of the valve leaflets.

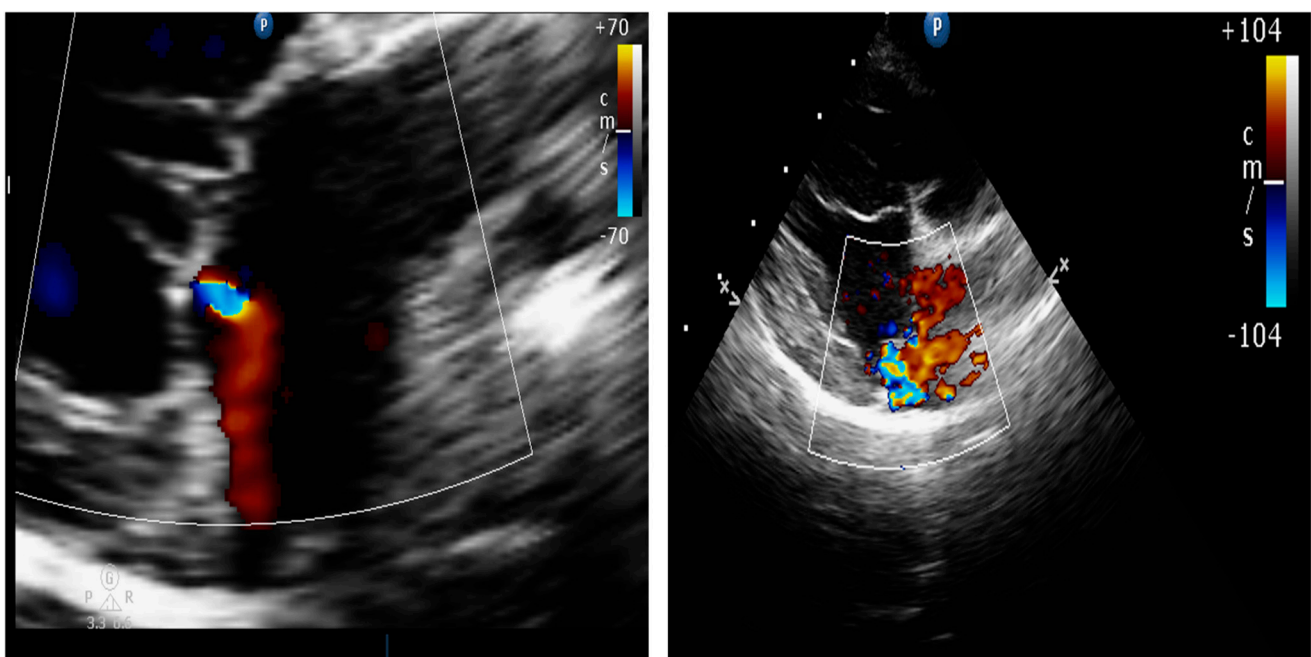


**Figure 8.** Mitral regurgitation in dogs due to myxomatous degeneration. Different degrees of valvular degeneration.

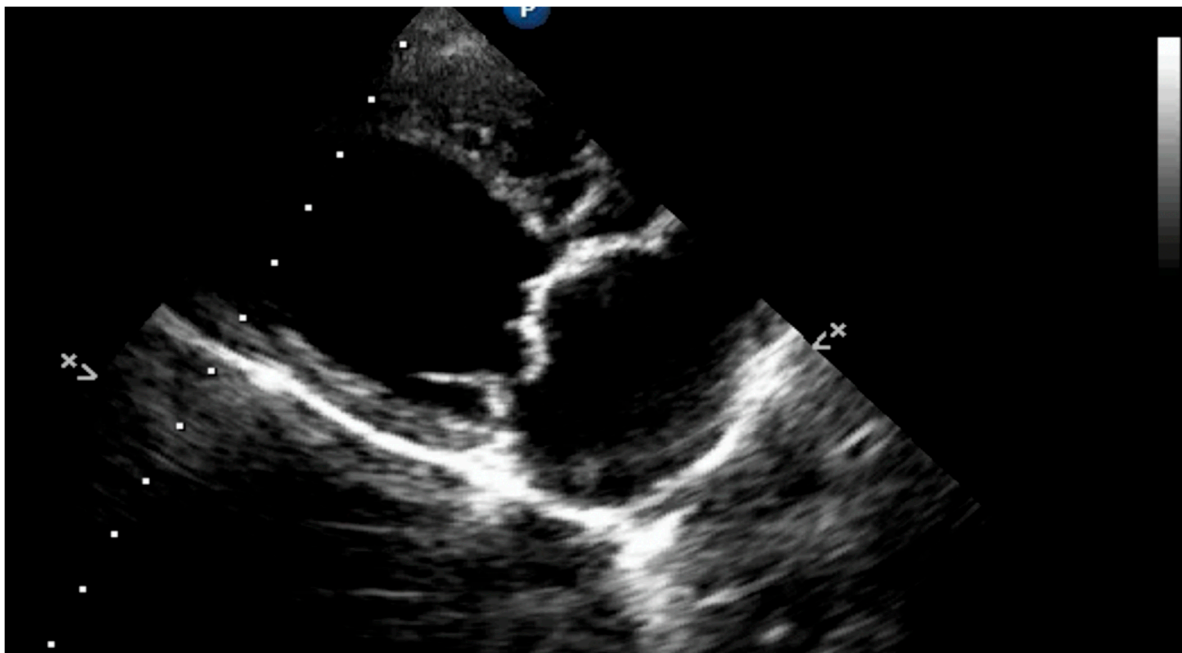


**Figure 9.** The presence of mitral valve septal leaflet prolapse is associated with tendinous chord rupture in the canine patient.

#### 5.7.5. Vmax Wave E

The maximum velocity of the E wave is influenced by atrial filling (preload) and the diastolic properties of the left ventricle, as shown in Figure 10. The maximum velocity of wave E tends to increase with preload, but only up to a certain point. The relaxation rate of the left ventricle decreases earlier in the development of congestive heart failure [54,67,85,90,91].

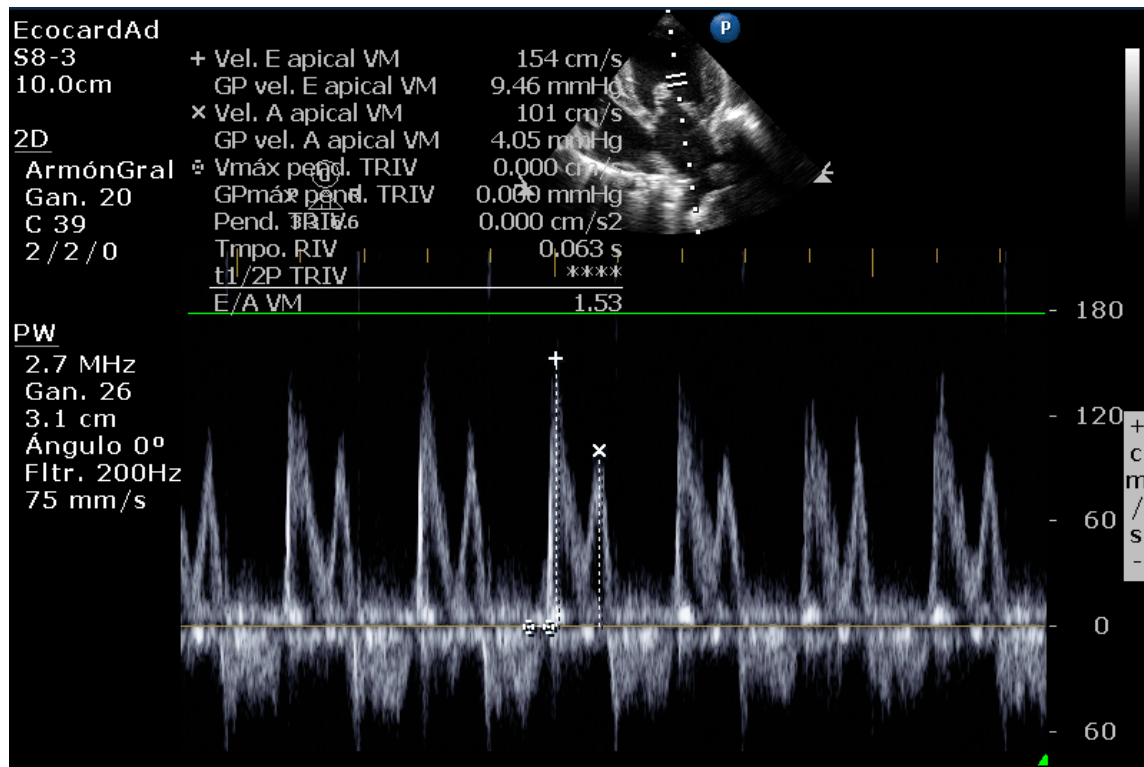


**Figure 10.** Transmitral Doppler shows increased E-wave velocity in a dog.

An E wave peak velocity greater than 1.2 m/s is associated with increased intra-atrial pressure; we can attribute the responsibility of pulmonary edema to the presence of congestive heart failure with values higher than these.

#### 5.7.6. E-Wave Deceleration Time

The literature review revealed that TDE is the parameter with the highest correlation with pulmonary capillary pressure in mitral regurgitation patients with systolic dysfunction. Values below 80 cm/sec are recognized as diminished [85,91,92].

#### 5.7.7. E/IVRT Ratio

An IVRT cutoff value  $< 45$  ms and  $E/IVRT > 2.5$  large diastolic filling pressures are seen as decisive in considering the possibility of congestive heart failure, as shown in Figure 11 [54,67,85,90,91,93].

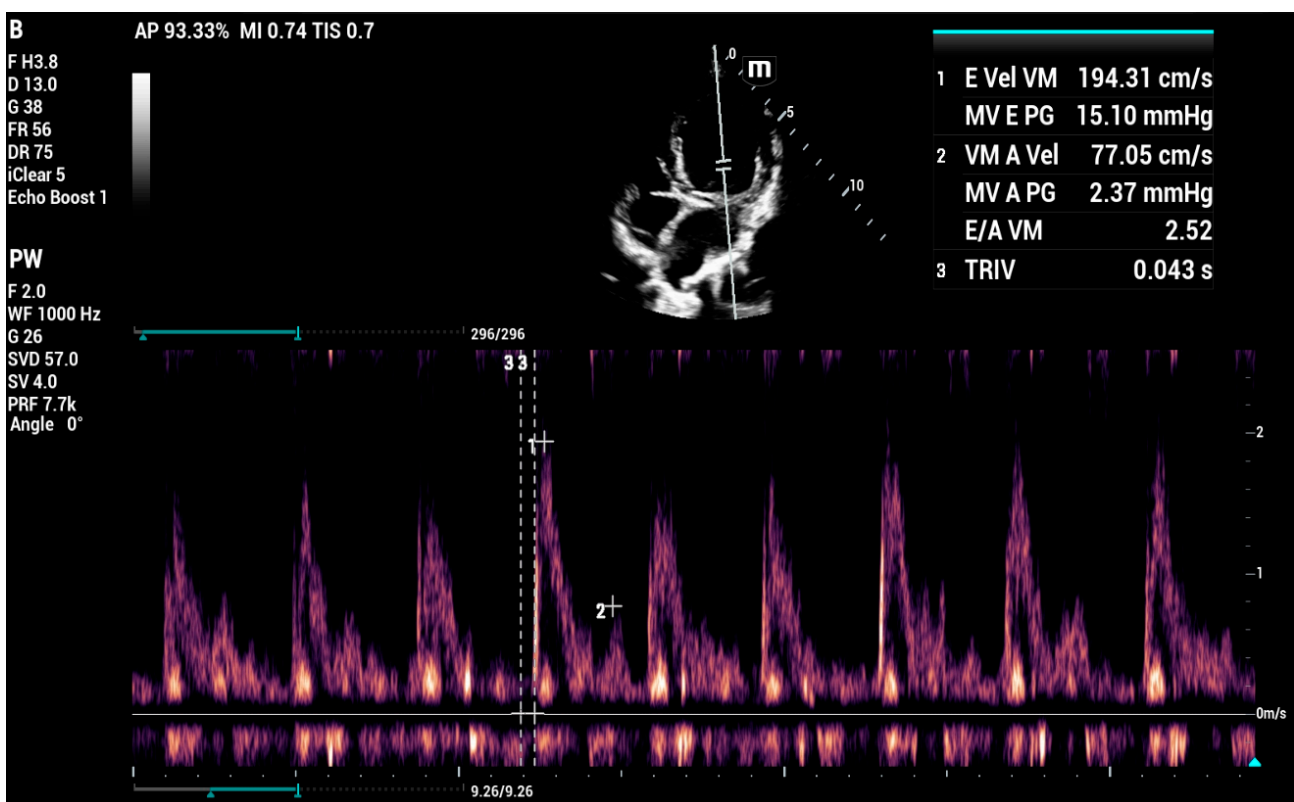


**Figure 11.** Increased E/IVRT ratio in a canine patient showing a restrictive pattern with mitral valve insufficiency and cardiogenic pulmonary edema.

#### 5.7.8. E/e' Ratio of the Mitral Annulus

An  $E/e' > 11.5$  in the case of patients with mitral valve insufficiency suggests an increase in the pressure of the pulmonary capillary above physiological levels, as shown in Figure 12. It generates the possibility of presenting congestive heart failure. A cardiogenic origin can be established in patients with pulmonary edema [53,67,85,90,91,93–95].

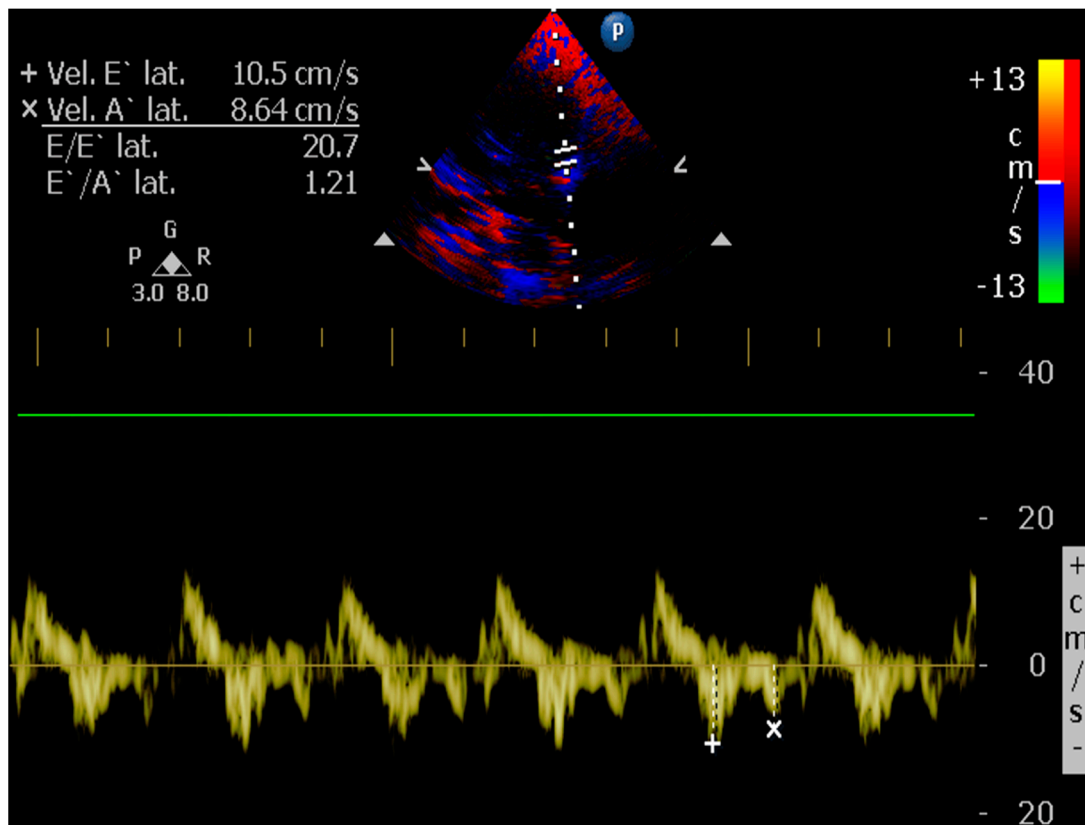


**Figure 12.** Altered E/e ratio in a canine patient with congestive heart failure.

## 6. Dilated Cardiomyopathy (DCM), a Human and Canine Common Disease

Cardiomyopathies are cardiac muscle disorders that could lead to mechanical and electrical heart malfunctions [96,97]. Cardiovascular disease is the fourth most common cause of death in dogs [98] and one of the most prevalent causes of death in humans [99]. Dilated cardiomyopathy (DCM) is the second most prevalent form of heart disease in domestic canines, accounting for 10% of heart disease in this species [97]. It is estimated to be the third most common hereditary heart disease in humans, affecting 35 patients in every 100,000, according to data that are considered underestimated [96].

Due to the similarities of DCM in humans and dogs regarding phenotypic characteristics and pathology progression, studies have suggested that canine MCD may act as a model for this pathology in humans. The above may apply to other fields, such as comparative clinical imaging research [100]. The scientific observation of the clinical course of this disease in the dog can guide improvements in clinical care and echocardiographic techniques in both canine and human patients.

Animal models of dilated cardiomyopathy are a useful research area because they can provide relevant information on the disease's cellular, structural, and hemodynamic progression, which is essential in improving treatment regimens [101], interventional procedures, and diagnostic imaging techniques. While there are many animal models in which dilated cardiomyopathy is induced, naturally occurring cases in dogs are particularly valuable concerning the disease's natural progression, especially when the underlying mechanisms are similar in dogs and people [96]. In addition to providing a potential natural model for human DCM in canines, it is potentially useful for studying new strategies and technologies for echocardiographic diagnosis in humans.

A significant association exists between dilated cardiomyopathy and congestive heart failure in dogs characterized by enlargement and impaired left ventricle contraction [96,102]. It is possible to classify dilated cardiomyopathy into three major stages [96]. At stage one, the heart appears normal, with no clinical evidence of cardiac disease, and often includes

dogs genetically predisposed to this pathology [96]. Stage two, classified as the preclinical or occult phase, involves morphologic and electrical changes in the heart, but with no overt clinical symptoms. Finally, stage three includes clinical signs of congestive heart failure [96].

The ideal standard approach for diagnosing DCM is based on 24 h echocardiographic and electrocardiographic (ECG) evaluations and monitoring the clinical presentation and patient progress [103]. In addition to a color Doppler echocardiographic evaluation, an electrocardiogram should also be performed simultaneously. The basic protocol includes all measurements performed in triplicate for volume and, ideally, five sequential cardiac cycles for M-mode testing [96]. Congenital or acquired heart disease other than DCM may also cause volume overload, systolic dysfunction, or both, and must be distinguished as a differential diagnosis in the dog. Volume overload in dogs can be caused by pathologies such as patent ductus arteriosus, ventricular septal defect, mitral valve dysplasia, and the myxomatous degeneration of the mitral valve [102].

### 6.1. Echocardiographic Measurements on DCM

Experience and clinical evidence point to TTE as a sensitive and specific medical resource in diagnosing dilated cardiomyopathy in dogs with congestive heart failure due to heart failure with reduced ejection fraction [104].

#### 6.1.1. Measurement of Left Ventricular Volume by Simpson's Method of Disks and Left Ventricular M-Mode

M-mode echocardiography is widely used in canine cardiology. Its one-dimensional nature limits the spatial information it provides, and the technique is based on geometric assumptions, which may vary according to the heart disease conditions, as shown in Figure 13 [102,103]. The American Society of Echocardiography recommends against using linear measurements to calculate left ventricular volume in the human patient and suggests that the biplanar Simpson's disk method (SMOD) is more suitable for this purpose [100]. Similarly, in a clinical study in dogs, the SMOD method was more sensitive than M-mode for detecting the presence of early echocardiographic changes, as shown in Figure 14a,b [96], and these results recommend that SMOD reference values should be used as a priority in the detection of early changes [103].

LV volume using the SMOD method is calculated in the right parasternal four-chamber long-axis view and in the left apical four-chamber view (in this technique, the aorta should not be visualized in either of these views), and it is important to trace the endocardial border in each image used. The image frame used to measure end-diastolic volume is selected by referencing the frames related to the onset of the QRS complex signaled by the synchronous electrocardiographic trace when the mitral valve is closed and the volume is at its peak. When measuring end-systolic volume in the heart, cardiologists choose the final frame just prior to the opening of the mitral valve. This is often the frame that follows the end of the T wave on an ECG and corresponds to a point in the cardiac cycle where volume is at its minimum. By selecting this specific frame, clinicians can obtain an accurate assessment of the heart's function. The right parasternal and left apical views should be measured, and larger volumes should be used, reducing the possibility of volume underestimation. It is important to note that the natural tendency for apical shortening in the heart can result in an underestimation of end-systolic and end-diastolic volumes. This phenomenon can complicate the interpretation of echocardiographic data [96].

The SMOD formula is a commonly used method to estimate left ventricular volume. This formula is based on tracing the endocardial border through the mitral valve annulus and measuring the longitudinal axis of the left ventricle. The left ventricular cavity is then divided into 20 disks of equal height to calculate the volume of the left ventricle. The cross-sectional area of each disk is determined by measuring the diameters of the left ventricle from two orthogonal views, which allows for a more accurate calculation of left ventricular volumes, and the end-diastolic (EDV) and end-systolic (ESV) volumes should be calculated

by the sum of the stacked disks, which is determined by the software of the current echocardiography equipment. The quantified volumes can be normalized concerning body surface area to obtain volume indices (EDV-I and ESV-I). Current guidelines indicate that an ESV-I greater than 80 mL/m<sup>2</sup> indicates systolic dysfunction [96,102]. Ejection fraction (EF) is calculated similarly to fractional shortening, but volume measurements are determined using the formula presented below:

$$EF = (EDV - ESV) / EDV \quad EF = EDV - ESV / EDV$$

Ejection fraction (EF) considers radial and longitudinal cardiac variations, and dogs with ejection fraction less than 40% are considered to have reduced contractile capacity [102].

### 6.1.2. E-Point to Septal Separation or EPSS: An Echocardiographic Parameter for Accurate Assessment of Left Ventricular Performance

The separation between the E point and the septum should be measured in the right parasternal long axis or the parasternal short axis at the level of the tip of the mitral septal leaflet. The separation between the E point and septum refers to the distance between the mitral septal leaflet’s peak early diastolic motion (E point) and the interventricular septum. A recent study in dogs evaluated EPSS as a technique for detecting occult dilated cardiomyopathy in Doberman canine patients. It demonstrated that EPSS greater than 6.5 mm is a valuable additional variable for diagnosing DCM. Incorporating the E point in the septal separation (EPSS) measurement, in addition to M-mode measurements, can enhance the sensitivity and specificity of cardiac evaluations, comparable to volume measurements obtained using the Simpson’s biplane method of disk summation or SMOD [96], as seen in Figure 15.

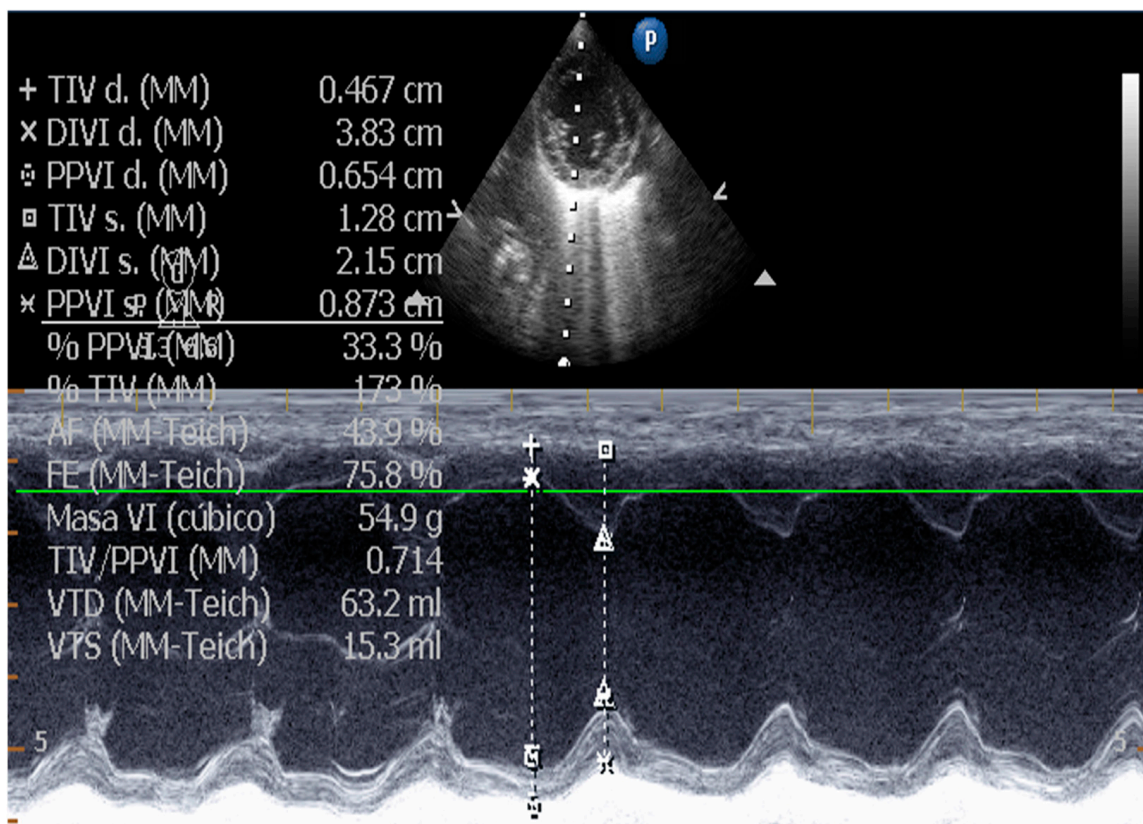
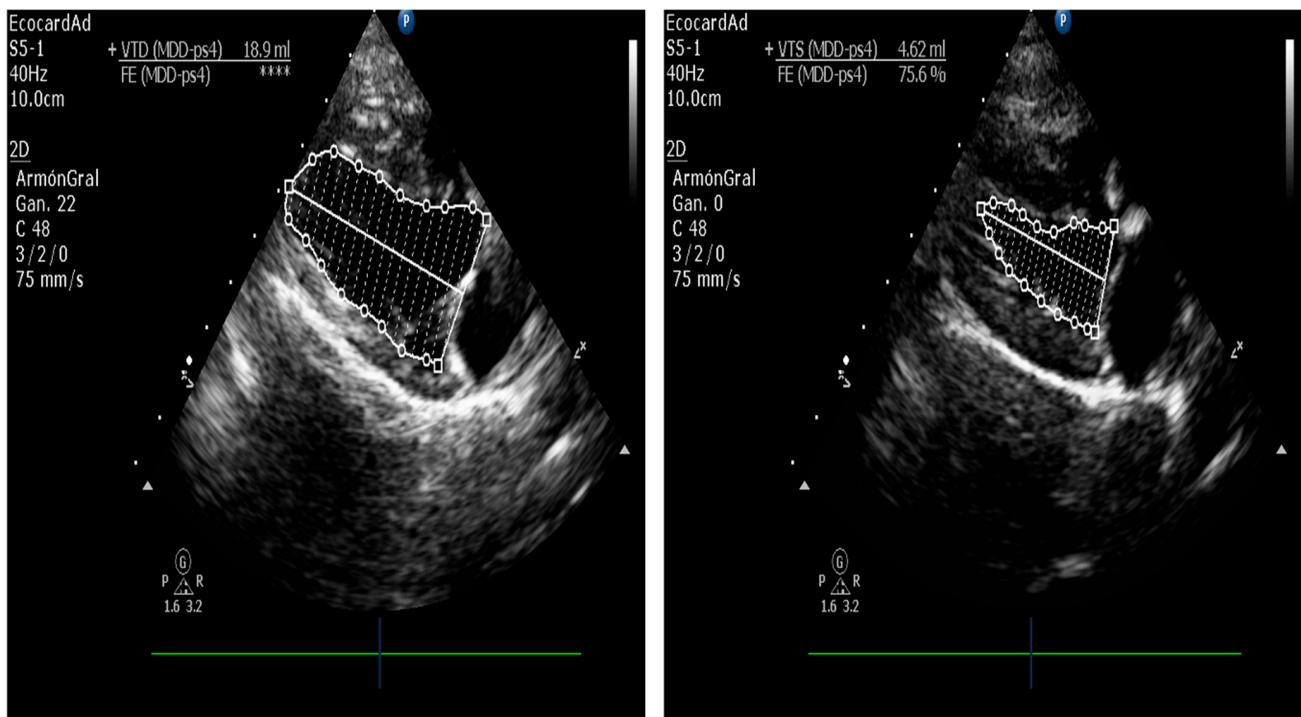


Figure 13. Left ventricular M-mode measurements in a dog.



(a)



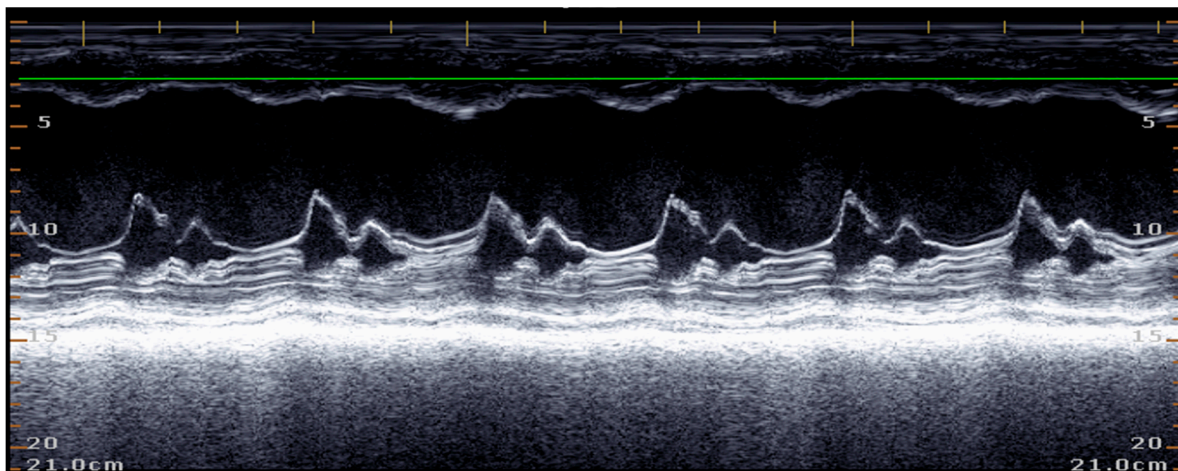
(b)

Figure 14. (a,b). Left ventricular volume by Simpson’s method of canine disk patient.

### 6.1.3. Sphericity Index (SI)

Assessing the left ventricle’s geometric shape or sphericity can be achieved by comparing the diastolic length. This measurement can be obtained from the right or left parasternal long axis views, as well as the apical four-chamber view acquired at end-diastole using the SMOD technique. However, it is crucial to exercise caution when measuring the apical LVIDD in M-mode to avoid any potential measurement-shortening. The Sphericity Index

is calculated by dividing the LV diastolic length by the left ventricular diastolic width at diastole. A Sphericity Index value less than 1.65 indicates increased sphericity and is considered abnormal according to the European Society of Veterinary Cardiology guidelines [45]. A study in dogs concluded that a value less than 1.65 is also the best cutoff point for identifying occult DCM in Doberman canine patients. However, it has been found that the sensitivity and specificity of SI, when used as the sole measure, is not sufficiently robust (sensitivity 86.8%, specificity 87.6%) compared to other standard volume estimates such as SMOD and EPSS. Due to the above points, its inclusion as a recommended parameter in standard monitoring protocols for dogs is not highly recommended, as shown in Figure 16a,b [96].



**Figure 15.** Increased mitral septal separation in a canine patient with DCM.

#### 6.1.4. Tissue Doppler and Speckle Tracking

Tissue Doppler imaging comprises several techniques such as tissue velocity imaging (TVI), strain, and strain rate imaging. Tissue velocity imaging allows for the assessment of the myocardial wall's early ( $a'$ ) and late ( $a'$ ) diastolic ( $e'$ ) and systolic ( $s'$ ) velocities using either pulsed wave or color Doppler myocardial echography [105].

TVI has demonstrated to be a promising technique for detecting early myocardial dysfunction in dogs with cardiomyopathy [105,106]. One study involving canine patients with either occult or overt dilated cardiomyopathy (DCM) demonstrated that the mitral annular velocities measured by pulsed-wave tissue velocity imaging were reduced in both systolic and diastolic phases [107]. In addition, a singular study investigated the systolic and diastolic tissue velocity imaging as well as strain parameters in canines diagnosed with Idiopathic Dilated Cardiomyopathy across different breeds [108].

In echocardiography, the assessment of myocardial deformation involves measuring the displacement and velocity of cardiac tissue during both systole and diastole. Strain refers to a dimensionless index of deformation that quantifies the percentage change in the length of a myocardial segment in the radial, circumferential, or longitudinal direction relative to the baseline measurement [109]. In contrast to tissue velocity imaging (TVI), strain and strain rate imaging are minimally influenced by the motion of the heart and tethering effects in adjacent segments. This overcomes the limitations of TVI and provides more accurate results. In human patients, these measurements have demonstrated high sensitivity in detecting myocardial diseases [110].

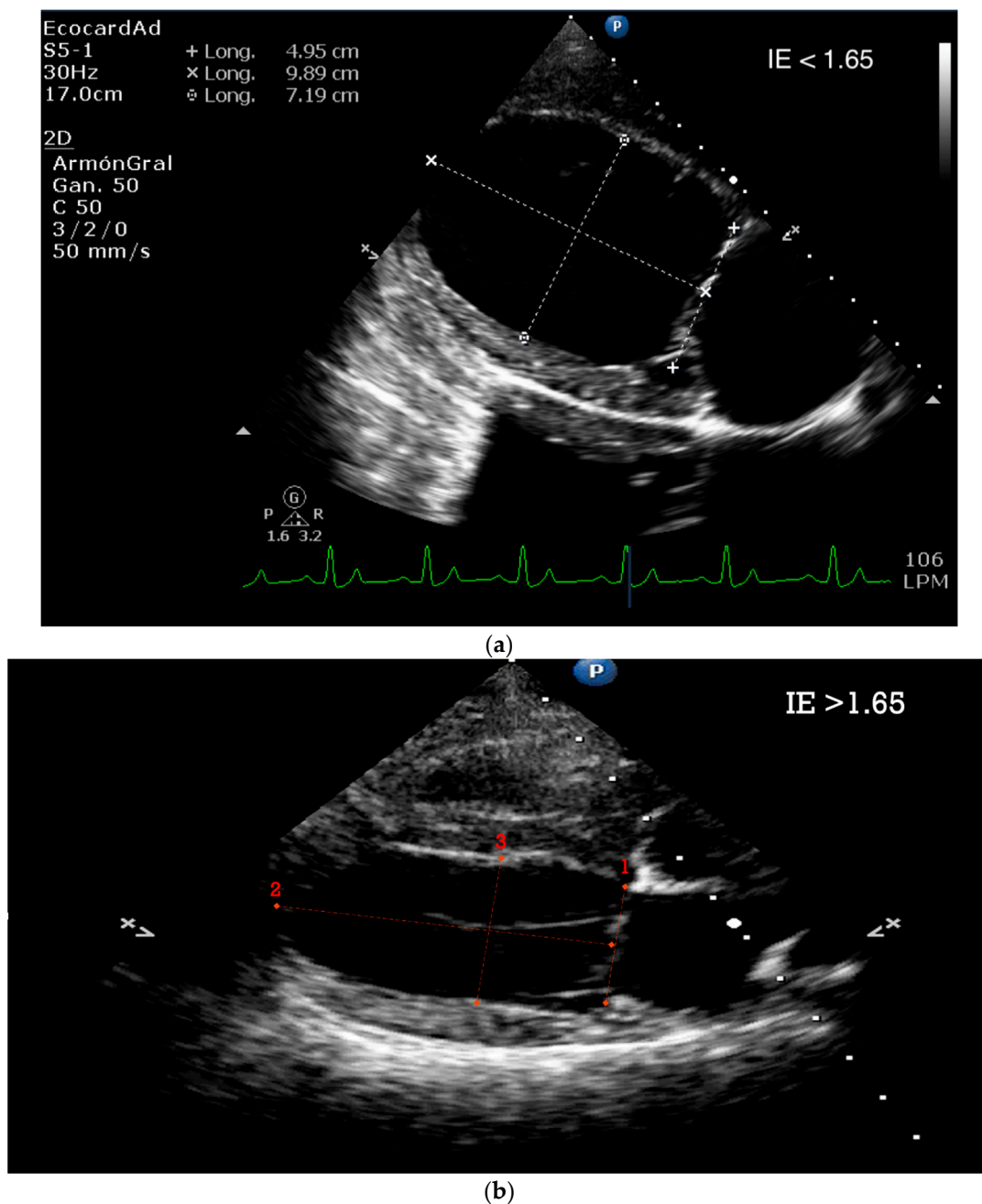


**Figure 16.** (a). Decreased Sphericity Index in canine patient. (b). Normal Sphericity Index in the canine patient.

### 7. Canine Patients with Naturally Occurring Cardiac Diseases—Learning from a Potential Echocardiography Research Model

Dogs have been an essential model for cardiology research since the beginning of experimental physiology in the nineteenth century, allowing the understanding of various mechanisms involved in the electrophysiological and mechanical functioning of the human heart [111]. Dogs' most common cardiovascular diseases, myxomatous mitral valve degeneration (MVD) and primary dilated cardiomyopathy (CMD), have an incidence of approximately 10% in daily canine veterinary clinical practice. In addition, the relatively short life span of dogs (12–14 years, depending on the breed) and the rapid evolution of these diseases turn the canine patient into a relevant clinical model for the comparative study of these same pathologies in humans [55,112].

In dogs, MVDM is the most common cardiovascular disease and has been associated with canine geriatric patients of certain dog breeds. In humans, its estimated prevalence is 2 to 3% of all cardiac diseases. The molecular and degenerative mechanisms involved in the evolution of the disease appear to be common in both species. For example, the migration of endothelial cells towards the interstitial tissue, stripping the valve's surface, characterizes the myxomatous degeneration of valve tissue in humans and canines [30].

For its part, CMD is the second most common cardiovascular disease in dogs. It develops from a preclinical or hidden phase, without obvious symptoms, up to a clinical-stage marked by congestive heart failure due to systolic dysfunction, severe arrhythmias, syncope, and even sudden death. In both canines and humans, it is associated with several genetic, inflammatory, and hemodynamic factors that cause a decrease in the contractile capacity of the myocardium and an increase in the internal diameter of the cardiac chambers [104,112].

Although murine models, mice, and rats have been used to study acute myocardial infarction and arterial hypertension, they have not been used to study these chronic diseases. In addition, these models face practical, technical, and scientific limitations inherent to the use of these species, for example: (a) The cardiovascular characteristics derived from their size, weight, and high metabolic rate make them very different from the human heart, especially in heart rate, oxygen consumption by the myocardium, contractility or inotropy, and response to drugs. (b) The difficult handling of these species makes them prone to stress during handling, with consequent cardiovascular physiological effects of elevated serum catecholamine levels. The tendency to develop arterial hypertension due to its management in the laboratory setting has made the murine model one of the most widely used models for the study of this condition, reaching the point of using hypertension induction methods that, in some cases, collide with important bioethical considerations regarding current scientific research. For example, arterial hypertension may be induced in rats that are semi-drowning in swimming pools which they cannot leave, meaning they must swim to survive, or hypertension may be induced by a combination of unilateral nephrectomy and a 10% sodium chloride solution orogastric tube [113]. (c) The need for aggressive manual or chemical containment employing sedation/anesthesia for clinical, electrocardiographic, and echocardiographic examination with the logical alterations of the cardiovascular variables to be evaluated, induced by the stress of handling or by the drugs used in the anesthetic plan. (d) The size of the murine models' hearts makes it difficult to obtain valid echocardiographic measurements, requiring special training for the staff, high-frequency ultrasound probes, and special adaptations of the software used for study interpretation. All of the above to make its implementation viable [114].

On the other hand, the dog, in its evolutionary process of more than 10,000 years accompanying the human being, has managed to adapt to its handling in such a way that, with minimum manual restraint (or sometimes without it), it tends to behave as an adequate clinical model, allowing painless procedures such as blood pressure measurement, electrocardiography, and echocardiography to be carried out without significant alterations, which will enable the evaluation of chronic diseases such as VMVD and CMD [111]. Furthermore, imaging acquisitions are ideal in cardiovascular disease animal models when performed with awake and cooperative animals, routinely performed in the dog during the follow-up of its cardiac pathology [5].

Echocardiography has become a systematic study in evaluating dogs' cardiovascular diseases because it is a minimally invasive procedure and is easily tolerated by dogs. Furthermore, the values obtained are reliable and repeatable since there is equipment adapted to the dogs' size and weight and computerized cardiology programs (software) adapted for the species, which correlate these values to the weight or body surface area of the patient, thus avoiding errors related to the variability of size, weight, and conformation of the thorax according to different breeds of dogs [101].

Currently, there are studies on dogs that show intervals or reference values, indexed to weight, breed, and even physical activity, for most of the normal echocardiographic

parameters for measuring size, contractility, and ejection of the cardiac chambers, degree of deformation of the walls, and the morphometric comparison of the various structures that make up the heart [115]. Likewise, canine echocardiography in its different modes (B, M, color or spectral Doppler, Tissue) allows us to evaluate the thickness, motility, and degree of competence of the heart valves, as well as the direction and speed of transvalvular blood flow, and calculate pressure gradients, the stage stenosis of the valves, or post-stenotic dilatations, among other parameters, in a reliable and repeatable way. This provides valuable information about the different stages through which dogs affected by these two diseases pass, allowing extrapolation of some of these findings to human pathology. Likewise, the relatively high incidence and prevalence in the population of these two canine diseases will enable the use of naturally affected patients as study models to evaluate both their evolution and the hemodynamic consequences derived from them, as well as the reaction to treatments [116].

Another advantage of using canine patients naturally affected by cardiac diseases as a comparative model in clinical imaging research is that these patients are diagnosed early in the course of the disease. Appropriate treatment is usually prescribed, allowing for the stable course of these pathologies in many cases, periodic evaluations of its evolution, and the determination of the effect of treatment on the disease and the survival period. Recently published studies, the EPIC study [79] and the BESST study [117], established an increase of up to 15 months in the preclinical stage of MMVD or Stage B2 in dogs (according to ACVIM consensus guidelines for the diagnosis and treatment of myxomatous mitral valve disease in dogs), allowing an adequate quality of life until the outcome of death or euthanasia associated with heart disease. This advantage enables a proper echocardiographic approach to these pathologies and an evaluation of the variations induced by current treatment.

Finally, the ideal animal model for studying human cardiac pathologies does not exist. However, the canine model appears to be appropriate for studying some chronic cardiac pathologies due to similarities in the neuroendocrine control of cardiac function, function, and expression of ion channels, hemodynamics, and even pharmacodynamics, in addition to the previously mentioned species and diseases. This is not the case for conditions with an acute and hyperacute course, such as myocardial infarction, since the coronary irrigation of the left ventricular myocardium in dogs is done through several collaterals of the main left coronary artery, compensating for the temporary ischemia of the infarcted tissue, modifying the course and intensity of the disease [111].

## 8. Conclusions

In cardiovascular research, animal models are essential for testing mechanistic hypotheses and insights and are relevant in translational research, the evaluation of medical procedures, and the development of imaging technologies.

There are many similarities between human and canine cardiac patients, including the cardiac anatomical structure, pathophysiological processes of some common myocardial and valvular diseases, and echocardiographic techniques used by both species, as shown in Table 1. Due to their remarkable similarity to the human heart, dogs are ideal models for studying ventricular function in heart failure models and improving echocardiographic assessment techniques and devices.

The present review proposes the canine patient with natural heart disease as a model for the clinical investigation of cardiac pathologies that are symmetric with those of the human patient. This is an excellent option in a current scenario, where continuous follow-up of cardiac disease in the dog is common, using technologies that allow for the measuring and monitoring of its evolution. In addition, the dog presents a particularity that we seek to point out; its short relative lifespan allows observing the behavior of these diseases in shorter periods than its human counterpart. Additionally, the current advanced veterinary cardiology and the highly manageable dog in the clinical context allow cardiac ultrasound studies without sedation or anesthesia, which is an advantage over other animal models. Observations from clinical echocardiography on dogs could improve our understanding

of cardiac disease, and canine models of human cardiac pathologies could supplement existing preclinical animal models.

**Table 1.** Comparison of Transthoracic Echocardiographic Techniques in Humans and Canines.

Technique	
Echocardiographic positioning	<b>Dogs</b> are usually imaged in right and left lateral position. The <b>human</b> patient should be supine or left lateral decubitus. This will bring the heart away from the sternum.
Normal Basic Echocardiographic Views	<b>Human:</b> Parasternal long axis, parasternal short axis, apical four chamber, apical four-chamber view, subxiphoid (subcostal), suprasternal view, and IVC views. <b>Canines:</b> Four-chamber right-sided parasternal long-axis view, five-chamber right-sided parasternal long-axis view, right-sided short-axis view of the left ventricle at the level of the papillary muscles, right-sided short-axis view at the level of the left atrium and aorta.
Quantitative assessment of mitral regurgitation	Commonly used in human patients, but seldom utilized in canine patients and practical application is limited (defining EROA and flow convergence shape can be challenging) [60].
Flow convergence area measurement by PISA	A standard gold method in <b>humans</b> , not routinely performed in cardiologic evaluation in <b>dogs</b> (PISA quantification showed a wide range of RF in a clinical study) [61,62].
Color flow imaging of the mitral regurgitation jet area	The most commonly used technique for assessing severity in <b>dogs</b> . The former method is not used in <b>humans</b> as it is not considered reliable for determining the severity of mitral insufficiency.
Measurement of Left Ventricular Volume	M-mode echocardiography is widely used in <b>canine</b> cardiology, but its utility is debated. American Society of Echocardiography recommends against using linear measurements in the <b>human</b> patient. SMOD is recommended [100,102,103].
Quantification of the severity of left ventricular remodeling	<b>Canine:</b> AI: Ao ratio, AI diameter indexed to weight, VI: Ao ratio, the normalized internal diameter of the VI at the end of normal diastole. Widely used. <b>Human:</b> Cardiovascular magnetic resonance is the gold standard and more accurate than echocardiography [118,119].

Our review has certain limitations. Narrative reviews are susceptible to selection bias, which is a disadvantage of this review genre. However, due to the novelty of the subject and the limited number of articles on the significance of using canine patients as a clinical model in echocardiographic translational research, other types of review systems may not be suitable. Our study provides a starting point for future investigations into the relevance of evaluating other echocardiographic techniques, such as transesophageal echocardiography and interventional imaging, in this topic. These areas should be the subject of future reviews to further advance our understanding of the topic.

This work does not propose using the canine patient as an experimental research model, which we believe will become increasingly obsolete due to its bioethical implications, but rather in the context of designing new echocardiographic technologies using interdisciplinary work and comparative and translational medical research. These comparisons could lead to the discovery of new echocardiographic diagnostic strategies to improve existing techniques and technologies, many of which could be tested on the dog. In addition, canine cardiac patients may provide clinically relevant models for relevant cardiovascular diseases of the heart in humans, and serve as a crucial link between preclinical echocardiographic research in naturally occurring disease models in dogs and clinical trials in human medicine. In this collaborative work, patients of both species could benefit from this combined interdisciplinary research effort.

Veterinary hospitals can provide excellent diagnostic and long-term medical care for canine pets, a basis for clinically relevant veterinary clinical trials. Translational research in canine patients with naturally occurring cardiac disease could strengthen the link between veterinary and human cardiac imaging research and feedback on the knowledge gained between the two disciplines.

**Author Contributions:** Conceptualization, C.A.F.D. and I.A.C.Y.; writing—original draft preparation, C.A.F.D., I.A.C.Y., R.M.G., J.C.H.R., M.F.M.G., S.M.G.C. and I.C.G.R.; writing—review and editing, C.A.F.D. and I.A.C.Y.; supervision, C.A.F.D.; project administration, C.A.F.D. All authors have read and agreed to the published version of the manuscript.

**Funding:** This research received no external funding.

**Institutional Review Board Statement:** Not applicable.

**Informed Consent Statement:** Not applicable.

**Data Availability Statement:** Not applicable.

**Acknowledgments:** The authors gratefully acknowledge Fernanda Reyna, Sergio Quintero, Efen Valenzuela, and the faculty and administrative personnel of the Veterinary Sciences Research Institute, Autonomous University of Baja California.

**Conflicts of Interest:** The authors declare no conflict of interest.

## References

- Roth, G.A.; Mensah, G.A.; Fuster, V. The Global Burden of Cardiovascular Diseases and Risks. *J. Am. Coll. Cardiol.* **2020**, *76*, 2980–2981. [[CrossRef](#)] [[PubMed](#)]
- Gaar-Humphreys, K.R.; Spanjersberg, T.C.F.; Santarelli, G.; Grinwis, G.C.M.; Szatmári, V.; Roelen, B.A.J.; Vink, A.; van Tintelen, J.P.; Asselbergs, F.W.; Fieten, H.; et al. Genetic Basis of Dilated Cardiomyopathy in Dogs and Its Potential as a Bidirectional Model. *Animals* **2022**, *12*, 1679. [[CrossRef](#)] [[PubMed](#)]
- Camacho, P.; Fan, H.; Liu, Z.; He, J.Q. Large Mammalian Animal Models of Heart Disease. *J. Cardiovasc. Dev. Dis.* **2016**, *3*, 30. [[CrossRef](#)] [[PubMed](#)]
- Löwa, A.; Jevtić, M.; Gorreja, F.; Hedtrich, S. Alternatives to animal testing in basic and preclinical research of atopic dermatitis. *Exp. Dermatol.* **2018**, *27*, 476–483. [[CrossRef](#)]
- Santos, A.; Fernández-Friera, L.; Villalba, M.; López-Melgar, B.; España, S.; Mateo, J.; Mota, R.A.; Jiménez-Borreguero, J.; Ruiz-Cabello, J. Cardiovascular imaging: What have we learned from animal models? *Front. Pharmacol.* **2015**, *6*, 227. [[CrossRef](#)]
- Demiris, G.; Oliver, D.P.; Washington, K.T. Defining and analyzing the problem. In *Behavioral Intervention Research in Hospice and Palliative Care*; Elsevier: Amsterdam, The Netherlands, 2019; pp. 27–39.
- Getty, R. General heart and blood vessels. In *Sisson and Grossman's: The Anatomy of the Domestic Animals*, 5th ed.; Sisson, S., Grossman, J.D., Getty, R., Eds.; Saunders: Philadelphia, PA, USA, 1975; pp. 164–175.
- Michaelsson, M.; Ho, S.Y. *Congenital Heart Malformations in Mammals: An Illustrated Text*; Imperial College Press: River Edge, NJ, USA; London, UK, 2000.
- Crick, S.J.; Sheppard, M.N.; Ho, S.Y.; Gebstein, L.; Anderson, R.H. Anatomy of the pig heart: Comparisons with normal human cardiac structure. *J. Anat.* **1998**, *193*, 105–119. [[CrossRef](#)]
- Queiroz, L.L.; Moura, L.R.; Moura, V.M.B.D. Morphometric assessment of canine heart without macroscopically visible changes caused by cardiac disease. *Ciênc. Anim. Bras.* **2018**, *19*, e43748. [[CrossRef](#)]
- Hill, A.J.; Laizzo, P.A. Comparative cardiac anatomy. In *Handbook of Cardiac Anatomy, Physiology, and Devices*; Iaizzo, P., Ed.; Humana Press: Totowa, NJ, USA, 2009. [[CrossRef](#)]
- Rodríguez, E.R.; Tan, C.D. Structure and Anatomy of the Human Pericardium. *Prog. Cardiovasc. Dis.* **2017**, *59*, 327–340. [[CrossRef](#)]
- Evans, H.E. The heart and arteries. In *Miller's Anatomy of the Dog*, 3rd ed.; Miller, M.E., Evans, H.E., Eds.; Saunders: Philadelphia, PA, USA, 1993; pp. 586–602.
- Holt, J.P. The normal pericardium. *Am. J. Cardiol.* **1970**, *26*, 455–465. [[CrossRef](#)]
- Naimark, W.A.; Lee, J.M.; Limeback, H.; Cheung, D.T. Correlation of structure and viscoelastic properties in the pericardia of four mammalian species. *Am. J. Physiol.* **1992**, *263*, H1095–H1106. [[CrossRef](#)]
- Spodick, D.H. *The Pericardium: A Comprehensive Textbook*; Dekker: New York, NY, USA, 1997.
- Czum, J.M.; Silas, A.M.; Althoen, M.C. Evaluation of the Pericardium with CT and MR. *ISRN Cardiol.* **2014**, *2014*, 174908. [[CrossRef](#)] [[PubMed](#)]
- Jakovljevic, D.G. Physical activity and cardiovascular aging: Physiological and molecular insights. *Exp. Gerontol.* **2018**, *109*, 67–74. [[CrossRef](#)]
- Singh, B. *Dyce, Sack, and Wensing's Textbook of Veterinary Anatomy*, 5th ed.; Elsevier: St. Louis, MO, USA, 2017.
- Walmsley, R. Anatomy of human mitral valve in adult cadaver and comparative anatomy of the valve. *Br. Heart J.* **1978**, *40*, 351–366. [[CrossRef](#)] [[PubMed](#)]
- Tarniceriu, C.C.; Hurjui, L.L.; Tanase, D.M.; Nedelcu, A.H.; Gradinaru, I.; Ursaru, M.; Stefan Rudeanu, A.; Delianu, C.; Lozneau, L. The Pulmonary Venous Return from Normal to Pathological—Clinical Correlations and Review of Literature. *Medicina* **2021**, *57*, 293. [[CrossRef](#)] [[PubMed](#)]
- Pettersson, G.B.; Hussain, S.T.; Ramankutty, R.M.; Lytle, B.W.; Blackstone, E.H. Reconstruction of fibrous skeleton: Technique, pitfalls and results. *Multimed. Man. Cardiothorac. Surg.* **2014**, *2014*, mmu004. [[CrossRef](#)]

23. Krawczyk-Ozóg, A.; Hołda, M.K.; Sorysz, D.; Koziej, M.; Siudak, Z.; Dudek, D.; Klimek-Piotrowska, W. Morphologic variability of the mitral valve leaflets. *J. Thorac. Cardiovasc. Surg.* **2017**, *154*, 1927–1935. [[CrossRef](#)] [[PubMed](#)]
24. Chen, Y.A.; Nguyen, E.T.; Dennie, C.; Wald, R.M.; Crean, A.M.; Yoo, S.J.; Jimenez-Juan, L. Computed tomography and magnetic resonance imaging of the coronary sinus: Anatomic variants and congenital anomalies. *Insights Imaging* **2014**, *5*, 547–557. [[CrossRef](#)]
25. Bigler, M.R.; Seiler, C. The Human Coronary Collateral Circulation, Its Extracardiac Anastomoses and Their Therapeutic Promotion. *Int. J. Mol. Sci.* **2019**, *20*, 3726. [[CrossRef](#)]
26. Teunissen, P.F.; Horrevoets, A.J.; van Royen, N. The coronary collateral circulation: Genetic and environmental determinants in experimental models and humans. *J. Mol. Cell. Cardiol.* **2012**, *52*, 897–904. [[CrossRef](#)]
27. Palmisano, A.; Nicoletti, V.; Colantoni, C.; Monti, C.B.; Pannone, L.; Vignale, D.; Darvizeh, F.; Agricola, E.; Schaffino, S.; De Cobelli, F.; et al. Dynamic changes of mitral valve annulus geometry at preprocedural CT: Relationship with functional classes of regurgitation. *Eur. Radiol. Exp.* **2021**, *5*, 34. [[CrossRef](#)]
28. Coutinho, G.F.; Antunes, M.J. Current status of the treatment of degenerative mitral valve regurgitation. *Rev. Port. Cardiol.* **2021**, *40*, 293–304. [[CrossRef](#)] [[PubMed](#)]
29. Neto, F.L.; Marques, L.C.; Aiello, V.D. Myxomatous degeneration of the mitral valve. *Autops. Case Rep.* **2018**, *8*, e2018058. [[CrossRef](#)] [[PubMed](#)]
30. Oyama, M.A.; Elliott, C.; Loughran, K.A.; Kossar, A.P.; Castellero, E.; Levy, R.J.; Ferrari, G. Comparative pathology of human and canine myxomatous mitral valve degeneration: 5HT and TGF- $\beta$  mechanisms. *Cardiovasc. Pathol.* **2020**, *46*, 107196. [[CrossRef](#)] [[PubMed](#)]
31. Merryman, W.D.; Youn, I.; Lukoff, H.D.; Krueger, P.M.; Guilak, F.; Hopkins, R.A.; Sacks, M.S. Correlation between heart valve interstitial cell stiffness and transvalvular pressure: Implications for collagen biosynthesis. *Am. J. Physiol. Heart Circ. Physiol.* **2006**, *290*, H224–H231. [[CrossRef](#)] [[PubMed](#)]
32. Sacks, M.S.; He, Z.; Baijens, L.; Wanant, S.; Shah, P.; Sugimoto, H.; Yoganathan, A.P. Surface strains in the anterior leaflet of the functioning mitral valve. *Ann. Biomed. Eng.* **2002**, *30*, 1281–1290. [[CrossRef](#)]
33. McCarthy, K.P.; Ring, L.; Rana, B.S. Anatomy of the mitral valve: Understanding the mitral valve complex in mitral regurgitation. *Eur. J. Echocardiogr.* **2010**, *11*, i3–i9. [[CrossRef](#)]
34. Fox, P.R. Pathology of myxomatous mitral valve disease in the dog. *J. Vet. Cardiol.* **2012**, *14*, 103–126. [[CrossRef](#)]
35. Markby, G.; Summers, K.M.; MacRae, V.E.; Del-Pozo, J.; Corcoran, B.M. Myxomatous degeneration of the canine mitral valve: From gross changes to molecular events. *J. Comp. Pathol.* **2017**, *156*, 371–383. [[CrossRef](#)]
36. Saremi, F.; Sánchez-Quintana, D.; Mori, S.; Muresian, H.; Spicer, D.E.; Hassani, C.; Anderson, R.H. Fibrous skeleton of the heart: Anatomic overview and evaluation of pathologic conditions with CT and MR imaging. *RadioGraphics* **2017**, *37*, 1330–1351. [[CrossRef](#)]
37. Jimenez, J.H.; Soerensen, D.D.; Zhaoming, H.; He, S.; Yoganathan, A.P. Effects of a saddle shaped annulus on mitral valve function and chordal force distribution: An in vitro study. *Ann. Biomed. Eng.* **2003**, *31*, 1171–1181. [[CrossRef](#)]
38. Padala, M.; Hutchison, R.A.; Croft, L.R.; Jimenez, J.H.; Gorman, R.C.; Gorman, J.H. Saddle shape of the mitral annulus reduces systolic strains on the P2 segment of the posterior mitral leaflet. *Ann. Thorac. Surg.* **2009**, *88*, 1499–1504. [[CrossRef](#)] [[PubMed](#)]
39. Connell, P.S.; Han, R.I.; Grande-Allen, K.J. Differentiating the aging of the mitral valve from human and canine myxomatous degeneration. *J. Vet. Cardiol.* **2012**, *14*, 31–45. [[CrossRef](#)] [[PubMed](#)]
40. Aupperle, H.; Disatian, S. Pathology, protein expression and signaling in myxomatous mitral valve degeneration: Comparison of dogs and humans. *J. Vet. Cardiol.* **2012**, *14*, 59–71. [[CrossRef](#)] [[PubMed](#)]
41. Combs, M.D.; Yutzey, K.E. Heart valve development: Regulatory networks in development and disease. *Circ. Res.* **2009**, *105*, 408–421. [[CrossRef](#)]
42. Ayoub, S.; Ferrari, G.; Gorman, R.C.; Gorman, J.H.; Schoen, F.J.; Sacks, M.S. Heart valve biomechanics and underlying mechanobiology. *Comp. Physiol.* **2016**, *6*, 1743–1780.
43. Nkomo, V.T.; Gardin, J.M.; Skelton, T.N.; Gottdiener, J.S.; Scott, C.G.; Enriquez-Sarano, M. Burden of valvular heart diseases: A population-based study. *Lancet* **2006**, *368*, 1005–1011. [[CrossRef](#)]
44. Marechaux, S.; Illman, J.E.; Huynh, J.; Michelena, H.I.; Nkomo, V.T.; Tribouilloy, C. Functional anatomy and pathophysiologic principles in mitral regurgitation: Non-invasive assessment. *Prog. Cardiovasc. Dis.* **2017**, *60*, 289–304. [[CrossRef](#)]
45. Aluru, J.S.; Barsouk, A.; Saginala, K.; Rawla, P.; Barsouk, A. Valvular Heart Disease Epidemiology. *Med. Sci.* **2022**, *10*, 32. [[CrossRef](#)]
46. Lung, B.; Vahanian, A. Epidemiology of valvular heart disease in the adult. *Nat. Rev. Cardiol.* **2011**, *8*, 162–172. [[CrossRef](#)]
47. Borgarelli, M.; Buchanan, J.W. Historical review, epidemiology and natural history of degenerative mitral valve disease. *J. Vet. Cardiol.* **2012**, *14*, 93–101. [[CrossRef](#)]
48. Parker, H.G.; Kilroy-Glynn, P. Myxomatous mitral valve disease in dogs: Does size matter? *J. Vet. Cardiol.* **2012**, *14*, 19–29. [[CrossRef](#)] [[PubMed](#)]
49. Lewis, T.W.; Wiles, B.M.; Llewellyn-Zaidi, A.M.; Evans, K.M.; O'Neill, D.G. Longevity and mortality in Kennel Club registered dog breeds in the UK in 2014. *Canine. Genet. Epidemiol.* **2018**, *5*, 10. [[CrossRef](#)] [[PubMed](#)]
50. Bagardi, M.; Bionda, A.; Locatelli, C.; Cortellari, M.; Frattini, S.; Negro, A.; Crepaldi, P.; Brambilla, P.G. Echocardiographic Evaluation of the Mitral Valve in Cavalier King Charles Spaniels. *Animals* **2020**, *10*, 1454. [[CrossRef](#)] [[PubMed](#)]

51. Hyun, C. Mitral valve prolapse in Cavalier King Charles spaniel: A review and case study. *J. Vet. Sci.* **2005**, *6*, 67–73. [[CrossRef](#)]
52. Enriquez-Sarano, M.; Michelena, H.I. Mitral regurgitation in the 21st century. *Prog. Cardiovasc. Dis.* **2017**, *60*, 285–288. [[CrossRef](#)]
53. Atkins, C.; Bonagura, J.; Ettinger, S.; Fox, P.; Gordon, S.; Haggstrom, J.; Hamlin, R.; Keene, B.; Luis-Fuentes, V.; Stepien, R. Guidelines for the diagnosis and treatment of canine chronic valvular heart disease. *J. Vet. Intern. Med.* **2009**, *23*, 1142–1150. [[CrossRef](#)]
54. Borgarelli, M.; Crosara, S.; Lamb, K.; Savarino, P.; La Rosa, G.; Tarducci, A.; Haggstrom, J. Survival characteristics and prognostic variables of dogs with preclinical chronic degenerative mitral valve disease attributable to myxomatous degeneration. *J. Vet. Intern. Med.* **2012**, *26*, 69–75. [[CrossRef](#)]
55. Keene, B.W.; Atkins, C.E.; Bonagura, J.D.; Fox, P.R.; Häggström, J.; Fuentes, V.L.; Oyama, M.A.; Rush, J.E.; Stepien, R.; Uechi, M. ACVIM consensus guidelines for the diagnosis and treatment of myxomatous mitral valve disease in dogs. *J. Vet. Intern. Med.* **2019**, *33*, 1127–1140. [[CrossRef](#)]
56. Boon, J.A. Acquired heart disease: Mitral insufficiency. In *Manual of Veterinary Echocardiography*, 1st ed.; Boon, J.A., Ed.; Williams and Wilkins: Baltimore, MD, USA, 1998; pp. 261–286.
57. Serres, F.; Chetboul, V.; Tissier, R.; Poujol, L.; Gouni, V.; Carlos Sampedrano CPouchelon, J.L. Comparison of 3 ultrasound methods for quantifying left ventricular systolic function: Correlation with disease severity and prognostic value in dogs with mitral valve disease. *J. Vet. Intern. Med.* **2008**, *22*, 566–577. [[CrossRef](#)]
58. Bonagura, J.D.; Schober, K.E. Can ventricular function be assessed by echocardiography in chronic canine mitral valve disease? *J. Small Anim. Pract.* **2009**, *50*, 12–24. [[CrossRef](#)]
59. Chetboul, V. Advanced techniques in echocardiography in small animals. *Vet. Clin. Small Anim. Pract.* **2010**, *40*, 529–543. [[CrossRef](#)] [[PubMed](#)]
60. Suh, S.-I.; Lu, T.-L.; Choi, R.; Hyun, C. Echocardiographic Features in Canine Myxomatous Mitral Valve Disease: An Animal Model for Human Mitral Valve Prolapse. In Proceedings of the Advanced Concepts in Endocarditis-2021, Virtual, 25 August 2021. [[CrossRef](#)]
61. Lancellotti, P.; Tribouilloy, C.; Hagendorff, A.; Popescu, B.A.; Edvardsen, T.; Pierard, L.A.; Badano, L.; Zamorano, J.L. Scientific document Committee of the European Association of cardiovascular imaging: Recommendations for the echocardiographic assessment of native valvular regurgitation: An executive summary from the European Association of Cardiovascular Imaging. *Eur. Heart J. Cardiovasc. Imaging* **2013**, *14*, 611–644. [[CrossRef](#)] [[PubMed](#)]
62. Gouni, V.; Serres, F.J.; Pouchelon, J.L.; Tissier, R.; Lefebvre, H.P.; Nicolle, A.P.; Sampedrano, C.C.; Chetboul, V. Quantification of mitral valve regurgitation in dogs with degenerative mitral valve disease by use of the proximal isovelocity surface area method. *J. Am. Vet. Med. Assoc.* **2007**, *231*, 399–406. [[CrossRef](#)]
63. Zoghbi, W.A.; Enriquez-Sarano, M.; Foster, E.; Grayburn, P.A.; Kraft, C.D.; Levine, R.A.; Nihoyannopoulos, P.; Otto, C.M.; Quinones, M.A.; Rakowski, H.; et al. Recommendations for evaluation of the severity of native valvular regurgitation with two-dimensional and Doppler echocardiography. *J. Am. Soc. Echocardiogr.* **2003**, *16*, 777–802. [[CrossRef](#)]
64. Chetboul, V.; Tissier, R. Echocardiographic assessment of canine degenerative mitral valve disease. *J. Vet. Cardiol.* **2012**, *14*, 127–148. [[CrossRef](#)] [[PubMed](#)]
65. Chetboul, V.; Serres, F.; Tissier, R.; Lefebvre, H.P.; Sampedrano, C.C.; Gouni, V.; Poujol, L.; Hawa, G.; Pouchelon, J.L. Association of plasma N-terminal pro-B-type natriuretic peptide concentration with mitral regurgitation severity and outcome in dogs with asymptomatic degenerative mitral valve disease. *J. Vet. Intern. Med.* **2009**, *23*, 984–994. [[CrossRef](#)]
66. Muzzi, R.A.; de Araújo, R.B.; Muzzi, L.A.; Pena, J.L.; Silva, E.F. Regurgitant jet area by Doppler color flow mapping: Quantitative assessment of mitral regurgitation severity in dogs. *J. Vet. Cardiol.* **2003**, *5*, 33–38. [[CrossRef](#)]
67. Sargent, J.; Muzzi, R.; Mukherjee, R.; Somarathne, S.; Schranz, K.; Stephenson, H.; Connolly, D.; Brodbelt, D.; Fuentes, V.L. Echocardiographic predictors of survival in dogs with myxomatous mitral valve disease. *J. Vet. Cardiol.* **2015**, *17*, 1–12. [[CrossRef](#)]
68. Grayburn, P.A.; Weissman, N.J.; Zamorano, J.L. Quantitation of mitral regurgitation. *Circulation* **2012**, *126*, 2005–2017. [[CrossRef](#)]
69. Zoghbi, W.A.; Adams, D.; Bonow, R.O.; Enriquez-Sarano, M.; Foster, E.; Grayburn, P.A.; Hahn, R.T.; Han, Y.; Hung, J.; Lang, R.M.; et al. Recommendations for non-invasive evaluation of native Valvular regurgitation: A report from the American Society of Echocardiography developed in collaboration with the Society for Cardiovascular Magnetic Resonance. *J. Am. Soc. Echocardiogr.* **2017**, *30*, 303–371. [[CrossRef](#)]
70. Vezzosi, T.; Grosso, G.; Tognetti, R.; Meucci, V.; Patata, V.; Marchesotti, F.; Domenech, O. The Mitral INsufficiency Echocardiographic score: A severity classification of myxomatous mitral valve disease in dogs. *J. Vet. Intern. Med.* **2021**, *35*, 1238–1244. [[CrossRef](#)] [[PubMed](#)]
71. Sargent, J.; Connolly, D.J.; Watts, V.; Mötsküla, P.; Volk, H.A.; Lamb, C.R.; Luis Fuentes, V. Assessment of mitral regurgitation in dogs: Comparison of results of echocardiography with magnetic resonance imaging. *J. Small Anim. Pract.* **2015**, *56*, 641–650. [[CrossRef](#)] [[PubMed](#)]
72. Biner, S.; Rafique, A.; Rafii, F.; Tolstrup, K.; Noorani, O.; Shiota, T.; Gurudevan, S.; Siegel, R.J. Reproducibility of proximal isovelocity surface area, vena contracta, and regurgitant jet area for assessment of mitral regurgitation severity. *JACC Cardiovasc. Imaging* **2010**, *3*, 235–243. [[CrossRef](#)] [[PubMed](#)]
73. Paiva, R.M.; Garcia-Guasch, L.; Manubens, J.; Montoya-Alonso, J.A. Proximal isovelocity surface area variability during systole in dogs with mitral valve prolapse. *J. Vet. Cardiol.* **2011**, *13*, 267–270. [[CrossRef](#)]

74. Tidholm, A.; Bodegård-Westling, A.; Höglund, K.; Häggström, J.; Ljungvall, I. Real-time 3-dimensional echocardiographic assessment of effective regurgitant orifice area in dogs with myxomatous mitral valve disease. *J. Vet. Intern. Med.* **2017**, *31*, 303–310. [[CrossRef](#)]
75. Borgarelli, M.; Savarino, P.; Crosara, S.; Santilli, R.A.; Chiavegato, D.; Poggi, M.; Bellino, C.; La Rosa, G.; Zanatta, R.; Haggstrom, J.; et al. Survival characteristics and prognostic variables of dogs with mitral regurgitation attributable to myxomatous valve disease. *J. Vet. Intern. Med.* **2008**, *22*, 120–128. [[CrossRef](#)]
76. Hansson, K.; Häggström, J.; Kwart, C.; Lord, P. Left atrial to aortic root indices using two-dimensional and M-mode echocardiography in cavalier King Charles spaniels with and without left atrial enlargement. *Vet. Radiol. Ultrasound* **2002**, *43*, 568–575. [[CrossRef](#)]
77. Cornell, C.C.; Kittleson, M.D.; Torre, P.D.; Häggström, J.; Lombard, C.W.; Pedersen, H.D.; Vollmar, A.; Wey, A. Allometric scaling of M-mode cardiac measurements in normal adult dogs. *J. Vet. Intern. Med.* **2004**, *18*, 311–321. [[CrossRef](#)]
78. Schober, K.E.; Hart, T.M.; Stern, J.A.; Li, X.; Samii, V.F.; Zekas, L.J.; Scansen, B.A.; Bonagura, J.D. Detection of congestive heart failure in dogs by Doppler echocardiography. *J. Vet. Intern. Med.* **2010**, *24*, 1358–1368. [[CrossRef](#)]
79. Boswood, A.; Häggström, J.; Gordon, S.G.; Wess, G.; Stepien, R.L.; Oyama, M.A.; Keene, B.W.; Bonagura, J.; MacDonald, K.A.; Patteson, M.; et al. Effect of pimobendan in dogs with preclinical myxomatous mitral valve disease and cardiomegaly: The EPIC study—A randomized clinical trial. *J. Vet. Intern. Med.* **2016**, *30*, 1765–1779. [[CrossRef](#)]
80. Reynolds, C.A.; Brown, D.C.; Rush, J.E.; Fox, P.R.; Nguyenba, T.P.; Lehmkühl, L.B.; Gordon, S.G.; Kellihan, H.B.; Stepien, R.L.; Lefbom, B.K.; et al. Prediction of first onset of congestive heart failure in dogs with degenerative mitral valve disease: The PREDICT cohort study. *J. Vet. Cardiol.* **2012**, *14*, 193–202. [[CrossRef](#)] [[PubMed](#)]
81. Dillon, A.R.; Dell’Italia, L.J.; Tillson, M.; Killingsworth, C.; Denney, T.; Hathcock, J.; Botzman, L. Left ventricular remodeling in preclinical experimental mitral regurgitation of dogs. *J. Vet. Cardiol.* **2012**, *14*, 73–92. [[CrossRef](#)]
82. Menciotti, G.; Borgarelli, M. Review of Diagnostic and Therapeutic Approach to Canine Myxomatous Mitral Valve Disease. *Vet. Sci.* **2017**, *4*, 47. [[CrossRef](#)]
83. McGinley, J.C.; Berretta, R.M.; Chaudhary, K.; Rossman, E.; Bratinov, G.D.; Gaughan, J.P.; Houser, S.; Margulies, K.B. Impaired contractile reserve in severe mitral valve regurgitation with a preserved ejection fraction. *Eur. J. Heart Fail.* **2007**, *9*, 857–864. [[CrossRef](#)]
84. Baron Toaldo, M.; Romito, G.; Guglielmini, C.; Diana, A.; Pelle, N.G.; Contiero, B.; Cipone, M. Prognostic value of echocardiographic indices of left atrial morphology and function in dogs with myxomatous mitral valve disease. *J. Vet. Intern. Med.* **2018**, *32*, 914–921. [[CrossRef](#)] [[PubMed](#)]
85. Lancellotti, P.; Pibarot, P.; Chambers, J.; La Canna, G.; Pepi, M.; Dulgheru, R.; Dweck, M.; Delgado, V.; Garbi, M.; Vannan, M.A.; et al. Multi-modality imaging assessment of native valvular regurgitation: An EACVI and ESC council of valvular heart disease position paper. *Eur. Heart J. Cardiovasc. Imaging* **2022**, *23*, e171–e232. [[CrossRef](#)] [[PubMed](#)]
86. Di Marcello, M.; Terzo, E.; Locatelli, C.; Palermo, V.; Sala, E.; Dall’Aglia, E.; Bussadori, C.M.; Spalla, I.; Brambilla, P.G. Assessment of mitral regurgitation severity by Doppler color flow mapping of the vena contracta in dogs. *J. Vet. Intern. Med.* **2014**, *28*, 1206–1213. [[CrossRef](#)] [[PubMed](#)]
87. Pedersen, H.D.; Häggström, J. Mitral valve prolapse in the dog: A model of mitral valve prolapse in man. *Cardiovasc. Res.* **2000**, *47*, 234–243. [[CrossRef](#)] [[PubMed](#)]
88. Nakamura, K.; Osuga, T.; Morishita, K.; Suzuki, S.; Morita, T.; Yokoyama, N.; Ohta, H.; Yamasaki, M.; Takiguchi, M. Prognostic value of left atrial function in dogs with chronic mitral valvular heart disease. *J. Vet. Intern. Med.* **2014**, *28*, 1746–1752. [[CrossRef](#)] [[PubMed](#)]
89. Wesselowski, S.; Borgarelli, M.; Menciotti, G.; Abbott, J. Echocardiographic anatomy of the mitral valve in healthy dogs and dogs with myxomatous mitral valve disease. *J. Vet. Cardiol.* **2015**, *17*, 97–106. [[CrossRef](#)]
90. Hezzell, M.J.; Boswood, A.; Moonarmart, W.; Elliott, J. Selected echocardiographic variables change more rapidly in dogs that die from myxomatous mitral valve disease. *J. Vet. Cardiol.* **2012**, *14*, 269–279. [[CrossRef](#)] [[PubMed](#)]
91. Kim, Y.H.; Choi, G.J.; Park, C. Rate of left ventricular pressure change by Doppler echocardiography in dogs with chronic mitral valve disease at different stages of congestive heart failure. *Vet. Radiol. Ultrasound* **2018**, *59*, 758–766. [[CrossRef](#)] [[PubMed](#)]
92. Chetboul, V.; Bussadori, C.; De Madron, É. *Clinical Echocardiography of the Dog and Cat*; Elsevier: Amsterdam, The Netherlands, 2016; pp. 127–138.
93. Kim, H.T.; Han, S.M.; Song, W.J.; Kim, B.; Choi, M.; Yoon, J.; Youn, H.Y. Retrospective study of degenerative mitral valve disease in small-breed dogs: Survival and prognostic variables. *J. Vet. Sci.* **2017**, *18*, 369–376. [[CrossRef](#)] [[PubMed](#)]
94. Kim, J.H.; Park, H.M. Usefulness of conventional and tissue Doppler echocardiography to predict congestive heart failure in dogs with myxomatous mitral valve disease. *J. Vet. Intern. Med.* **2015**, *29*, 132–140. [[CrossRef](#)] [[PubMed](#)]
95. Santos, M.; Rivero, J.; McCullough, S.D.; West, E.; Opotowsky, A.R.; Waxman, A.B.; Systrom, D.M.; Shah, A.M. E/e’ Ratio in Patients with Unexplained Dyspnea: Lack of Accuracy in Estimating Left Ventricular Filling Pressure. *Circ. Heart Fail.* **2015**, *8*, 749–756. [[CrossRef](#)]
96. Simpson, S.; Kordtomeikel, K.; Wong, S.; Bennison, S.; El-Gendy, S.A.; Cobb, M.; Rutland, C.S. Diagnosis, Prognosis, Management, Treatment, Research and Advances in Canine Dilated Cardiomyopathy. In *Canine Genetics, Health and Medicine*; Rutland, C., Ed.; IntechOpen: London, UK, 2021; Available online: <https://www.intechopen.com/chapters/76601> (accessed on 17 November 2022). [[CrossRef](#)]

97. Egenvall, A.; Bonnett, B.N.; Häggström, J. Heart Disease as a Cause of Death in Insured Swedish Dogs Younger than 10 Years of Age. *J. Vet. Intern. Med.* **2006**, *20*, 894–903. [[CrossRef](#)] [[PubMed](#)]
98. Fleming, J.M.; Creevy, K.E.; Promislow, D.E. Mortality in north american dogs from 1984 to 2004: An investigation into age-, size-, and breed-related causes of death. *J. Vet. Intern. Med.* **2011**, *25*, 187–198. [[CrossRef](#)]
99. Mathers, C.D.; Loncar, D. Projections of global mortality and burden of disease from 2002 to 2030. *PLoS Med.* **2006**, *3*, e442. [[CrossRef](#)]
100. Mausberg, T.B.; Wess, G.; Simak, J.; Keller, L.; Drögemüller, M.; Drögemüller, C.; Webster, M.T.; Stephenson, H.; Dukes-McEwan, J.; Leeb, T. A locus on chromosome 5 is associated with dilated cardiomyopathy in Doberman Pinschers. *PLoS ONE* **2011**, *6*, e20042. [[CrossRef](#)]
101. Dixon, J.A.; Spinale, F.G. Large animal models of heart failure: A critical link in the translation of basic science to clinical practice. *Circ Heart Fail.* **2009**, *2*, 262–271. [[CrossRef](#)]
102. Wess, G.; Domenech, O.; Dukes-McEwan, J.; Häggström, J.; Gordon, S. European Society of Veterinary Cardiology screening guidelines for dilated cardiomyopathy in Doberman Pinschers. *J. Vet. Cardiol.* **2017**, *19*, 405–415. [[CrossRef](#)] [[PubMed](#)]
103. Wess, G.; Schulze, A.; Butz, V.; Simak, J.; Killich, M.; Keller, L.J.; Maeurer, J.; Hartmann, K. Prevalence of dilated cardiomyopathy in doberman pinschers in various age groups. *J. Vet. Intern. Med.* **2010**, *24*, 533–538. [[CrossRef](#)] [[PubMed](#)]
104. Bonagura, J.D.; Visser, L.C. Echocardiographic assessment of dilated cardiomyopathy in dogs. *J. Vet. Cardiol.* **2022**, *40*, 15–50. [[CrossRef](#)] [[PubMed](#)]
105. Wess, G.; Killich, M.; Hartmann, K. Comparison of pulsed wave and color Doppler myocardial velocity imaging in healthy dogs. *J. Vet. Intern. Med.* **2010**, *24*, 360–366. [[CrossRef](#)]
106. Chetboul, V.; Carlos, C.; Blot, S.; Thibaud, J.L.; Escriou, C.; Tissier, R.; Retortillo, J.L.; Pouchelon, J.L. Tissue Doppler assessment of diastolic and systolic alterations of radial and longitudinal left ventricular motions in Golden Retrievers during the preclinical phase of cardiomyopathy associated with muscular dystrophy. *Am. J. Vet. Res.* **2004**, *65*, 1335–1341. [[CrossRef](#)]
107. O’Sullivan, M.L.; O’Grady, M.R.; Minors, S.L. Assessment of diastolic function by Doppler echocardiography in normal Doberman Pinschers and Doberman Pinschers with dilated cardiomyopathy. *J. Vet. Intern. Med.* **2007**, *21*, 81–91. [[CrossRef](#)]
108. Chetboul, V.; Gouni, V.; Sampedrano, C.C.; Tissier, R.; Serres, F.; Pouchelon, J.L. Assessment of regional systolic and diastolic myocardial function using tissue Doppler and strain imaging in dogs with dilated cardiomyopathy. *J. Vet. Intern. Med.* **2007**, *21*, 719–730. [[CrossRef](#)]
109. Klæboe, L.G.; Edvardsen, T. Echocardiographic assessment of left ventricular systolic function. *J. Echocardiogr.* **2019**, *17*, 10–16. [[CrossRef](#)]
110. Dandel, M.; Hetzer, R. Echocardiographic strain and strain rate imaging—clinical applications. *Int. J. Cardiol.* **2009**, *132*, 11–24. [[CrossRef](#)]
111. Loen, V.; Vos, M.A.; van der Heyden, M.A.G. The canine chronic atrioventricular block model in cardiovascular preclinical drug research. *Br. J. Pharmacol.* **2022**, *179*, 859–881. [[CrossRef](#)]
112. Japp, A.G.; Gulati, A.; Cook, S.A.; Cowie, M.R.; Prasad, S.K. The Diagnosis and Evaluation of Dilated Cardiomyopathy. *J. Am. Coll. Cardiol.* **2016**, *67*, 2996–3010. [[CrossRef](#)] [[PubMed](#)]
113. Romero Borges, R.; Valido Díaz, A.; Bernal Llerenas, T.; Fimia Duarte, R.; Iannacone, R. Biomodel of arterial hypertension in Wistar rats administered 10% saline solution. *Biotempo* **2018**, *15*, 75–82.
114. Zaragoza, C.; Gomez-Guerrero, C.; Martin-Ventura, J.L.; Blanco-Colio, L.; Lavin, B.; Mallavia, B.; Tarin, C.; Mas, S.; Ortiz, A.; Egido, J. Animal models of cardiovascular diseases. *J. Biomed. Biotechnol.* **2011**, *2011*, 497841. [[CrossRef](#)] [[PubMed](#)]
115. Esser, L.C.; Borkovec, M.; Bauer, A.; Häggström, J.; Wess, G. Left ventricular M-mode prediction intervals in 7651 dogs: Population-wide and selected breed -specific values. *J. Vet. Intern. Med.* **2020**, *34*, 2242–2252. [[CrossRef](#)]
116. de Madron, É. Normal Views: 2D, TM, Spectral, and Color Doppler. In *Clinical Echocardiography of the Dog and Cat*; Chetboul, V., Bussadori, C., de Madron, É, Eds.; Elsevier Publishing: St. Louis, MO, USA, 2016.
117. Coffman, M.; Guillot, E.; Blondel, T.; Garelli-Paar, C.; Feng, S.; Heartsill, S.; Atkins, C.E. Clinical efficacy of a benazepril and spironolactone combination in dogs with congestive heart failure due to myxomatous mitral valve disease: The BENazepril Spironolactone Study (BESST). *J. Vet. Intern. Med.* **2021**, *35*, 1673–1687. [[CrossRef](#)]
118. Bellenger, N.G.; Burgess, M.I.; Ray, S.G.; Lahiri, A.; Coats, A.J.; Cleland, J.G.; Pennell, D.J. Comparison of left ventricular ejection fraction and volumes in heart failure by echocardiography, radionuclide ventriculography and cardiovascular magnetic resonance. Are they interchangeable? *Eur. Heart J.* **2000**, *21*, 1387–1396. [[CrossRef](#)]
119. Grothues, F.; Smith, G.C.; Moon, J.C.; Bellenger, N.G.; Collins, P.; Klein, H.U.; Pennell, D.J. Comparison of interstudy reproducibility of cardiovascular magnetic resonance with two-dimensional echocardiography in normal subjects and in patients with heart failure or left ventricular hypertrophy. *Am. J. Cardiol.* **2002**, *90*, 29–34. [[CrossRef](#)]

**Disclaimer/Publisher’s Note:** The statements, opinions and data contained in all publications are solely those of the individual author(s) and contributor(s) and not of MDPI and/or the editor(s). MDPI and/or the editor(s) disclaim responsibility for any injury to people or property resulting from any ideas, methods, instructions or products referred to in the content.